

**Reduction of nitroarenes using carbon supported cobalt
phosphide as a catalyst**



By

Ayesha Arif

MS Chemistry-2022

Reg No. 403048

Supervisor

Dr Manzar Sohail

Department of Chemistry

School of Natural Sciences (SNS)

National University of Sciences and Technology (NUST), Islamabad

October, 2024

**Reduction of nitroarenes using carbon supported cobalt
phosphide as a catalyst**

By

Ayesha Arif

MS Chemistry-2022

Reg no. 403048

A thesis submitted in partial fulfillment of the requirements for the degree

of

MS Chemistry

Thesis Supervisor:

Dr Manzar Sohail

Department of Chemistry

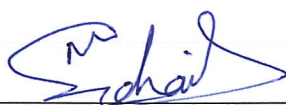
School of Natural Sciences (SNS)

National University of Sciences and Technology (NUST), Islamabad

October 2024

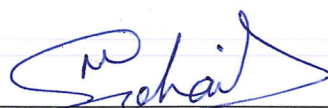
THESIS ACCEPTANCE CERTIFICATE

Certified that final copy of MS thesis written by Ayesha Arif (Registration No. 00000403048), of School of Natural Sciences has been vetted by undersigned, found complete in all respects as per NUST statutes/regulations, is free of plagiarism, errors, and mistakes and is accepted as partial fulfillment for award of MS/M.Phil degree. It is further certified that necessary amendments as pointed out by GEC members and external examiner of the scholar have also been incorporated in the said thesis.

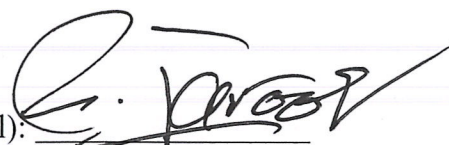
Signature:  _____

Name of Supervisor: Prof. Manzar Sohail _____

Date: 20/11/2024 _____

Signature (HoD):  _____


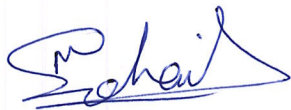
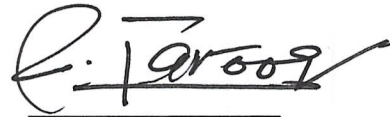
Date: 20/11/2024 _____

Signature (Dean/Principal):  _____

Date: 20-11-2024 _____

National University of Sciences & Technology**MS THESIS WORK**

We hereby recommend that the dissertation prepared under our supervision by: Ayesha Arif, Regn No 00000403048 Titled Reduction of Nitro Aromatic Compounds be Accepted in partial fulfillment of the requirements for the award of MS degree.

Examination Committee Members1. Name: PROF. MUHAMMAD ARFANSignature: 2. Name: DR. KHADIJA MUNAWARSignature: Supervisor's Name PROF. MANZAR SOHAILSignature: Head of Department20/11/2024Date**COUNTERSIGNED**20.11.2024DateDean/Principal

*Dedicated to my exceptional parents and adored siblings whose
tremendous support and cooperation led me to this wonderful
accomplishment.*

Acknowledgement

I am thankful to my Creator Allah Subhana-Watala to have guided me throughout this work at every step and for every new thought which You setup in my mind to improve it. Indeed, I could have done nothing without Your priceless help and guidance. Whosoever helped me throughout the course of my thesis, whether my parents or any other individual, was Your will, so indeed none be worthy of praise but You.

I am profusely thankful to my beloved parents who raised me when I was not capable of walking and continued to support me throughout every department of my life. They made it possible for me to reach where I am today.

I would also like to express special thanks to my supervisor Dr Manzar Sohail for his help throughout my thesis and also for topics in inorganic chemistry course which he has taught me. I can safely say that I haven't learned any other subject in such depth than the ones which he has taught.

I would also like to thank Dr Muhammad Arfan and Dr Khadija Munawar for being on my thesis guidance and evaluation committee. I also thank all the individuals who have rendered valuable assistance to my study.

I would also like to pay special thanks to Sara Zainab for teaching me and her tremendous support and cooperation. Each time I got stuck in something; she came up with the solution. I would also like to give special thanks to Anosha Rubab for all her help. Without their help I wouldn't have been able to complete my thesis. I appreciate their patience and guidance throughout the whole thesis.

I am also greatly thankful to Aamal Rehaman and Aqsa Shabbir for their immense support and keeping me motivated during my research phase.

Ayesha Arif

Table of Contents

1	ABSTRACT.....	x
2	Chapter 1.....	1
2.1	INTRODUCTION	1
2.2	Why transition metal phosphide (TMP)?.....	2
2.3	Transition metal phosphide's applications.....	2
2.4	Why Amines?.....	4
2.5	Synthesis methods.....	6
2.5.1	Decomposition of metal-organic precursors	6
2.5.2	Gas-solid phase reaction	6
2.5.3	Solid-state reaction.....	7
2.5.4	Solvothermal/hydrothermal route	7
2.5.5	High energy ball mining	8
2.5.6	Electrodeposition method	8
2.5.7	Chemical deposition method.....	8

2.6	Characterization Techniques.....	9
2.6.1	X-Ray Diffraction (XRD).....	9
2.6.2	Raman Spectroscopy.....	12
2.6.3	Fourier Transform Infrared Spectroscopy (FTIR).....	15
2.6.4	Scanning electron microscopy (SEM).....	16
2.6.5	Transmission electron microscopy (TEM).....	18
3	Chapter 2.....	21
3.1	Literature Review.....	21
4	Chapter 3.....	30
4.1	Methodology.....	30
4.1.1	Cobalt-TPP synthesis.....	30
4.1.2	Cobalt-TPP deposition on AC.....	31
4.1.3	Decomposition pf Cobalt-TPP complex.....	31
4.2	Chemical Equation.....	32
5	Chapter 4.....	33
5.1	Characterization.....	33

5.1.1	X-Ray Diffraction	33
5.1.2	Raman Spectroscopy.....	34
5.1.3	Fourier-Transform Infrared Spectroscopy (FTIR).....	35
5.1.4	Scanning Electron Microscopy	36
5.1.5	Elemental Disruptive Spectroscopy	37
5.1.6	Transmission Electron Microscopy	37
5.2	Application.....	40
5.2.1	Optimization reactions using catalytic reduction of nitrobenzene.....	41
5.2.2	Catalytic reduction of p-Nitrobiphenyl.....	43
5.2.3	Catalytic reduction of different substrates at 25 bar:	45
6	Conclusion	53
7	References.....	54

List of Figures

Figure 1 Wavelength distribution of radiation produced by sealed tube and rotating anode (2)	10
Figure 2 Schematic representation of working principle of X-ray Diffraction	11
Figure 3 Raman Spectroscopy instrumentation	13
Figure 4 Schematic representation of working principle of Raman Spectroscopy.....	14
Figure 5 FTIR instrumentation	15
Figure 6 Scanning Electron Microscopy instrumentation	17
Figure 7 Transmittance Electron Microscopy instrumentation	20
Figure 8 Synthesis of CoP@N dopped C	22
Figure 9 CoP@OMC used as bifunctional material for HER and ESC.....	24
Figure 10 Synthesis of Co ₃ P using red phosphorous	25
Figure 11 Structure of hyperbranched Co ₂ P nanocrystals	26
Figure 12 Reduction of nitroarenes to aniline.....	27
Figure 13 Synthesize of Cobalt phosphide using ZIF-67 and red phosphorus	27

Figure 14 Schematic diagram for Co-TPP complex synthesis	30
Figure 15 Schematic diagram for deposition of Co-TPP complex on activated carbon	31
Figure 16 Pyrolysis of complex to gain <i>Co₂P/C</i>	32
Figure 17 Proposed reaction for the synthesis of <i>Co₂P</i>	32
Figure 18 pXRD spectrum of <i>Co₂P/C@800</i> , <i>Co₂P/C@600</i> and <i>Co₂P/C@400</i>	34
Figure 19 Raman spectra of <i>Co₂P/C@800</i>	35
Figure 20 FTIR spectra of <i>Co₂P/C@800</i>	36
Figure 21 Scanning electron microscopy image of <i>Co₂P/C@800</i> at a) $5\mu\text{m}$ and b) $2\mu\text{m}$	36
Figure 22 EDS spectrum of <i>Co₂P/C@800</i>	37
Figure 23 TEM image of <i>Co₂P/C@800</i> at 10nm	38
Figure 24 HRTEM image of <i>Co₂P/C@800</i> at 10nm	39
Figure 25 Schematic diagram for nitroarene molecular hydrogenation	40
Figure 26 Gas Chromatogram of Aniline at a) 15 bar and b) at 25 bar	42
Figure 27 MS spectra of Aniline.....	42
Figure 28 Gas Chromatograph of p-Aminobiphenyl.....	44

Figure 29 MS spectra of p-Aminobiphenyl	44
Figure 30 Gas Chromatogram of 4-Aminoacetophenone at 25 bar.....	46
Figure 31 MS spectra of 4-Aminoacetophenone	47
Figure 32 Gas Chromatogram of 3-Aminobenzonitrile at 25bar.....	48
Figure 33 MS spectra of 3-Aminobenzonitrile	48
Figure 34 Gas Chromatogram of 2-Amino-5-bromopyridine at 25bar	49
Figure 35 MS spectra of 2-Amino-5-bromopyridine.....	50

ABSTRACT

Catalysis has played an important role in various fields such as batteries, water splitting, environment protection, energy storage, chemical synthesis and many others in the past decades. An example is using catalyst in the field of hydrogenating nitroarenes. Nitroarenes hold great importance due to their use in pharmaceuticals, agriculture, dyes etc. This process of reduction usually requires harsh conditions. Moreover, in this work the target catalyst is cobalt phosphide whose synthesis usually requires not only high temperature and long hours but also an inert environment. So, in this thesis cobalt phosphide nanoparticles deposited on activated carbon (Co_2P/C) are synthesized and used to selectively reduce nitroarenes by molecular hydrogenation. The synthesis of Co_2P/C is through decomposition of the organic complex. A complex of Co-TPP was made via solution method which is then pyrolyzed to produce Co_2P/C . The characterization of the catalyst prepared was done using XRD, SEM, Raman, TEM, and FTIR. Co_2P/C then effectively catalyzes the reduction of nitroarenes to amines in conditions that are mild.

Chapter 1

1.1 Introduction

A major field in chemistry is catalysis, about 90% of the chemical reactions involve the use of catalysts in one step at the least [1]. Heterogeneous catalysis in particular is the backbone of industries, both chemical and energy due to the high capability to accelerate reactions, low cost, product selectivity, high conversion rates and recyclability. Therefore, the demand of catalyst is at an increase due to the increasing demands in energy, synthetic products, food as well as the demand to deal with the increasing levels of CO_2 [2, 3].

The ultimate goal is to design and create a cost-effective, green and high-quality catalyst with great efficiency. Artificially built nanostructures, particularly supported metal nanoparticles, are utilized to enhance the efficiency of catalyst and overcome the barrier of energy. However, metal nanoparticles suffer from air stability and require pretreatment due to which alloying with other metals or non-metals, controlling morphology and doping with heteroatoms is carried out to increase not only the activity but also the stability of catalyst [4, 5].

Recently, phosphorous alloying with transition metals, which is generally known as transition metal phosphides (TMP), in particular is merging as a favorable plan for smart catalysts [6]. These catalyst show high activity and superior air stability for environmental friendly and efficient hydrogenation reactions. Moreover P-alloying also not only increase the density of the d-electron in metal which facilitates hydrogenation but also favors selective reaction [4].

Additionally, many phosphides of non-noble metal such as Ni_2P , NiP , Co_2P , CoP , Fe_2P , etc. have been tested as suitable alternatives for noble metal-based catalyst for many reactions related to industry.

1.2 Why transition metal phosphide (TMP)?

TMP are formed when metal or semimetal are combined with phosphorous. The crystal structures might have binary, secondary or high-order structure which can be ionic as well as other complex structures. The bonding also varies by varying composition and constitution of elements, it can be covalent, metallic or ionic. The ratio between the metal and phosphorous can vary making the compound either metal rich, phosphorous rich or stoichiometric phosphide. The properties of TMP also vary according to the composition. For instance, metal rich and stoichiometric phosphide have strong M-P have high thermal stability, hardness, resistance to chemical attack and oxidation. On the other hand, phosphorous rich form oligomers, chains, planes and clusters. They have comparatively lower thermal stability, are softer and have higher reactivity. Depending on these properties TMP are used in various applications [7]. TMP have surfaces as an efficient catalyst due to its unique electronic and catalytic properties [8].

1.3 Transition metal phosphide's applications

Energy conservation, storage and alternate fuel sources are rising issues due to the current energy crisis. TMP plays a role in all three of the fields due to its characteristics structural as well as chemical properties [8].

One of the important functions of TMP is in storage of energy, because of its low cost along with its high storage capacity, in both rechargeable Li-ion batteries [9] [10] and supercapacitor. Metal phosphides, have high electronic conductivity and show little change in volume during charge-discharge process. This along with their capacity and suitable voltage for open circuit make them a great fit for Li-ion batteries [11]. Moreover due to their thermal stability and resistance they are used for making of stable electrode in supercapacitor as the specific supercapacitance is seen to have increased by the use of nanosheets of metal phosphides [12].

Another important application of TMP is in photocatalytic and electrocatalytic oxidation and reduction. One of the most common electrochemical applications is water splitting. TMP plays an outstanding role in both OER and HER process due to the interaction of phosphorous and the intermediates formed during reaction, which forms surface structures appropriate for hydride and proton receptor sites. Moreover, due to their catalytic activity, eco-friendly and availability along with bifunctional properties they have been extensively used [13].

The electrochemical [14] and photochemical [15] water splitting produces hydrogen gas that is one of the sustainable sources of energy and is in high-demand [16]. Moreover the reactions of evolution of oxygen (OER) and reduction of oxygen (ORR) are processes used commonly in metal-air batteries [17] and fuel cell.

Another photochemical activity of TMP is the use in solar cells. Photovoltaics are a promising renewable source of energy that can help meet the increasing demand of energy. TMP due to their

high catalytic activity, long stability and great conductivity have been commonly used in solar cells to generate energy [18].

TMPs are also used in the field of sensors. They have been used as both biosensors to sense glucose [19], dopamine [20] etc. and chemo sensors for food analysis [21], gas analysis [22] etc. TMP have been used as sensors due to their abundance, tunable electronic structures and their unique physiochemical properties. Moreover, their good sensing is due to their stability and high selectivity to particular compounds.

They are also used in heterocatalysis due to their excellent selectivity and catalytic activity they are used to reduce nitroarenes to amines which are greatly used in different industries such as pharmaceutical [23]. Similarly, they are also used in the reduction of CO_2 gas. The effect of global warming has cause the focus to shift to a method to reduce CO_2 production and increase its removal and one of the ways is the reduction for which TMP are greatly tested [24].

All these applications depends upon the unique characteristics that changes by changing composition, structure and synthesis methods.

1.4 Why Amines?

Amines belong to the group in which the compounds contain sp_3 hybridized nitrogen atom. Ammonia NH_3 is the simplest amine present. Replacing the hydrogen in ammonia with other elements will result in inorganic salts like NCl_3 while replacing it with carbon chain will produce an organic compound. The carbon chain can be an alkyl chain forming alkyl amine or it can be an

aryl chain forming aryl amine. Moreover, the number of hydrogens replaced can also vary forming 3 categories of amines.

- Replacing one hydrogen with an alkyl or aryl group gives a primary (1°) alkyl or aryl amine. This has the formula $R - NH_2$ and over here the R in the formula can be any alkyl group or it can be an aryl group.
- Replacing two hydrogen with an alkyl or aryl group gives a secondary (2°) alkyl or aryl amine. This can be represented by $R' - NH - R''$ where R' and R'' can be same groups or different groups.
- Replacing three hydrogen with an alkyl or aryl group gives a tertiary (3°) alkyl or aryl amine.. It is represented by $R - NR'_2$ where one or all three carbon groups can be different [25].

Amines are vastly used in different fields of sciences including materials, biology, chemistry, medicine and environment. They are used as precursors or as intermediates in different synthesis of chemicals or in pharmaceuticals, agriculture field, polymers etc. Majorly they are present in biomolecules therefore are greatly used in drugs. In 200 top drugs sold in 2018 about 48% of them had either amine or other nitrogen containing molecule in them [26]. In short amines hold great importance and an easy method to synthesis these amines is through reducing the nitroarenes.

1.5 Synthesis methods

1.5.1 Decomposition of metal-organic precursors

For this, an organic source of phosphorous, like trioctylphosphine (TOP), triphenyl phosphite (TPOP) etc is mixed with a source of metal either metal nanoparticles, metal oxide, metal salt, metal carbonyl or a bulk metal etc to produce metal-organic precursor. These metal-organic precursors are then thermally decomposed at a high temperature of 250-300°C and inert environment to produce TMPs. Altering the concentration of metal and phosphorous precursors changed the metal/phosphorous ratio in the desired product. Similarly varying the temperature can give a variety of crystalline phases of TMPs [27].

1.5.2 Gas-solid phase reaction

Another method of synthesizing TMP is by gas-solid phase reaction. In this phosphorus source is in gas phase. PH_3 is active in phosphorization but it is lethal. Phosphine can also be produced by the decomposition of salts like hypophosphite such as NaH_2PO_2 and $\text{NH}_4\text{H}_2\text{PO}_2$, at 250 °C or higher temperatures. Phosphine gas reacts with metal in form of either oxides (MO), organic frameworks or hydroxides (MOH) to form TMP at different temperatures. This method surfactants are not used and therefore the product is able to uphold its morphology and proportions but is not preferred due to its toxicity. Post treatment of the tail gas will be needed in this method [28].

1.5.3 Solid-state reaction

Solid phase phosphidation is another method of synthesizing TMPs. Here metal precursor used is a solid, such as oxides, hydroxides, or nanoparticles of metals, is combined with a source of phosphorus which is also a solid, like red phosphorous, followed by decomposition at high temperatures in argon or nitrogen environment. This is also a temperature sensitive reaction, therefore the phase of the product changes by changing the temperature. Li et al. synthesized Nickel phosphide. At 275 °C, pure Ni_2P phase was formed but as temperature was increased Ni_5P_4 and NiP_2 phases dominate. At 325°C Ni_5P_4 was purely formed. Changing the ratio between the metal and phosphorous precursors also produces diversity in crystalline phases of TMPs also effecting the shapes and sizes [29].

1.5.4 Solvothermal/hydrothermal route

Hydrothermal reaction is carried out in water. The metal and phosphorous precursor is dissolved in water by stirring then transferred to a Teflon autoclave and sealed. It is then kept at high temperature (120–200 °C) for a certain time. It was later cooled and to get precipitates which are washed and dried [30]. On other hand solvothermal method uses organic solvent such as oleyl amine and 1-octadecene as a reaction medium. The structure and morphology of the TMP varies depending upon the nucleation process which can be controlled by the temperature, the stoichiometric ratio between metal and phosphorous and the precursor [29].

1.5.5 High energy ball mining

This is an effective process of producing nanoscale particles from bulk material. It produces a blend of various phases [31]. This process is not restricted to a specific metal precursor but can be used for synthesis of monometallic, bimetallic TMPs. Black phosphorous obtained by grinding red phosphorous at room temperature is grounded with metal precursor to obtain TMPs [32]. Ball mining utilizes the rotation and vibration of the grinding material such as steel balls and pebbles to fuse the material [33].

1.5.6 Electrodeposition method

Electrodeposition is a efficient and cost-effective method compared to other techniques and provides versatility as it allows the material to deposit directly on substrates like carbon cloth, nickel foam, PET and titanium plate etc. This allows the formation of huge surface area that is electrically active and allows better conductivity along with stable interfaces [34]. A solution containing metal ions and phosphorous source like hypophosphite ions are used. When current is passed the electrons get accumulated on the substrate surface. The ions react with electrons on the surface and are reduces forming atoms of metal and phosphorous. These are deposited on the substrate and fuse with each other forming TMPs[35].

1.5.7 Chemical deposition method

This method is widely used in producing a thin film that are made on heated substrates by reaction using gas precursors. It has 3 components: energy source, vacuum system and exhaust system. The

energy source provides the necessary heat or energy to break down the precursor materials introduced into the system. This energy can be supplied in various forms, including thermal heating or plasma energy, depending on the specific CVD method employed. After introducing the precursors, the vacuum system plays a critical role by removing undesired gaseous species from the reaction chamber. This step is essential to maintain the purity of the environment in which the chemical reactions occur. Finally, the exhaust system is responsible for eliminating volatile byproducts generated during the deposition process. This ensures that harmful gases are safely removed from the system, thereby enhancing safety and efficiency [36]. For this method first the metal precursor is synthesized using hydrothermal method and deposited on substrate or thin film. Then by phosphorization the metal precursor is converted to TMPs. But this process has drawbacks, such as irregular deposition on substrate, high temperature and production of toxic gas as red phosphorous is used for phosphorization [37].

1.6 Characterization Techniques

1.6.1 X-Ray Diffraction (XRD)

XRD has the capability to supply details about the structure and identity of the matter including arrangement of atoms, inter-atomic distances, particle size, bond angles and electron distribution of atoms etc. [38].

X-rays are generated by sealed tubes or rotating anodes. Rotating anodes along with sealed tubes produce both Bremsstrahlung, x-rays with broad continuous distribution of wavelength, as well as

characteristic radiation of the target material. XRD method only uses K_{α} radiation which are the characteristic radiation of the material with the highest intensity, rest of the radiations are filtered out using appropriate filter materials [39].

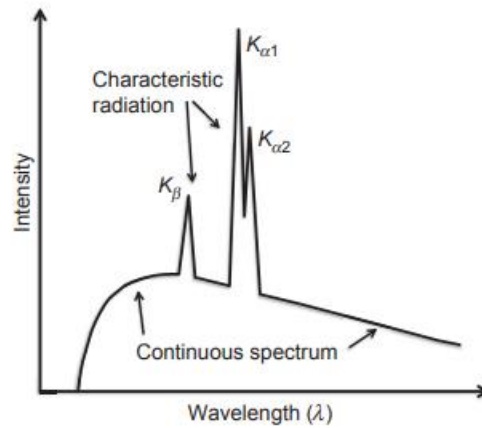


Figure 1 Wavelength distribution of radiation produced by sealed tube and rotating anode (2)

The XRD works of Bragg's law that states that a constructive interference is produced when the following condition is satisfied on the interaction of incident rays and the sample:

$$n\lambda = 2d\sin\theta$$

where 'n' stands for an integer, 'λ' for wavelength, 'd' for interplanar spacing and 'θ' for the angle of diffraction.

Bragg's law relates wavelength of the x-ray, angle of diffraction and sample's lattice spacing. To analyze rays diffracted are detected, processed and counted. Scanning from different 2θ angles

all possible diffraction direction can be obtained which on conversion to the d-spacing helps in identification as compounds usually have their own d-spacing unique to them [40].

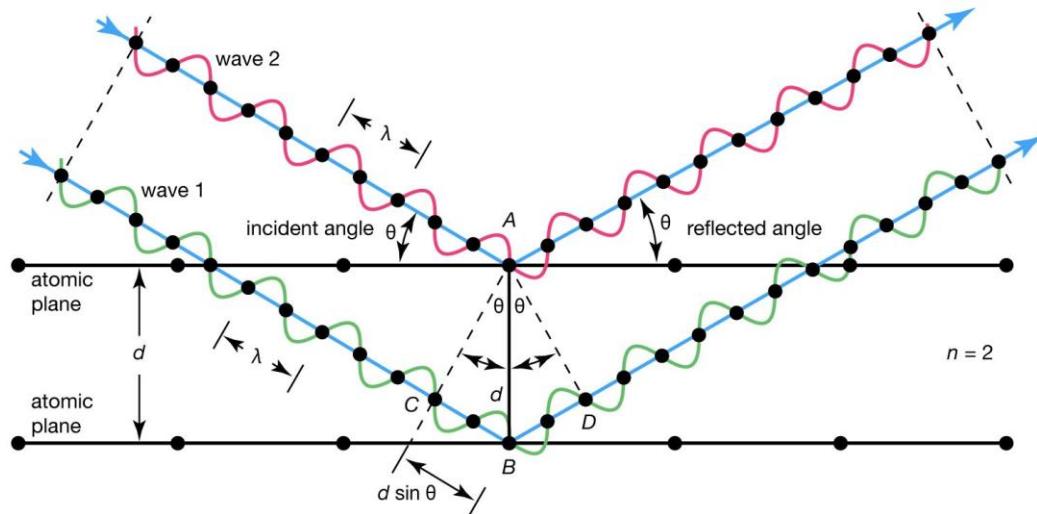


Figure 2 Representation of X-ray Diffraction's working principles

XRD peak size gives information about the crystallite size. Broad peak shows decrease in the crystallite size from bulk to nanoscale. Debye Scherrer equation is used to quantitatively describe the size of the crystallite.

$$D = \frac{k\lambda}{\beta \cos\theta}$$

Where k stands for Scherrer constant, shape factor constant, D for particle size, λ for incident rays wavelength, θ for angle of diffraction and β for the peak's FWHM (full width half maximum) [41].

1.6.2 Raman Spectroscopy

This tool was first theoretically predicted by Semkal (1923) and experimented by Krishnan (1928). It is a branch of vibrational spectroscopy, that helps in the interpretation and identification of trace chemicals depending on their vibrations. The vibrational characteristics of a chemical are unique and are also called its fingerprints [42].

This technique uses high energy photons in the near IR and visible region.

The Raman effect happens because the light interacts with the vibrations caused by the chemical bonds of the substance. At a microscopic level the effect happens due to the light falling on the electron density of bond causing excitation on vibrational level of molecule and change in the frequency of the light. Thus, a fingerprint region of vibrations of molecule unique to it is obtained which helps in the identification and characterization [43].

The spectrometer is made of a source of light, a monochromator, a sample holder and finally a detector.

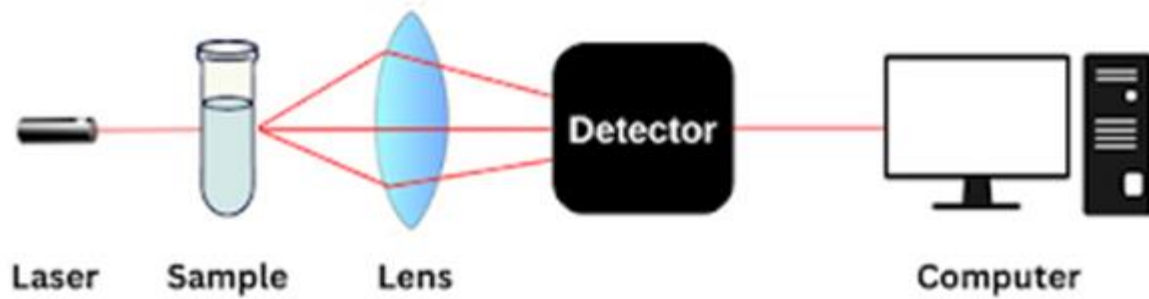


Figure 3 Raman Spectroscopy instrumentation

There are 2 main types of Raman Scattering: Elastic and Inelastic. In elastic scattering shift in the frequency or wavelength of photon does not appears. While in the inelastic scattering the frequency and wavelength change are observed [42].

Inelastic can be further divided to two types: Stroke and Anti-stroke Raman scattering. In strokes the light scattered has longer wavelength that means it has less energy than the incident light. This is because the sample absorbing energy from the incident light raises in the vibrational energy level. In anti-Stokes the light scattered has shorter wavelength that means it has higher energy. This is because the sample absorbing energy from the incident light will lose the energy to the incident light in this situation [44].

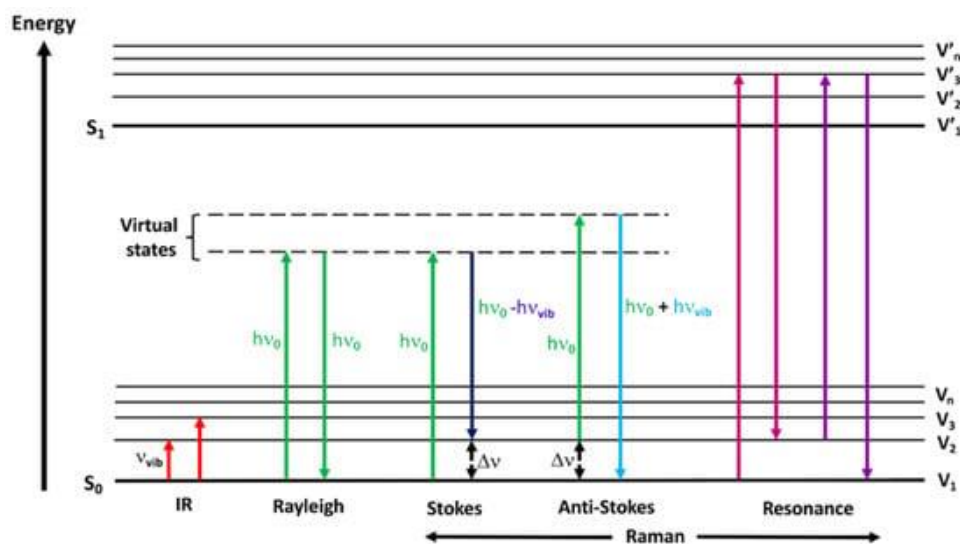


Figure 4 Schematic representation of working principle of Raman Spectroscopy

Diagnostic application: Raman spectroscopy helps in distinguishing between a cancerous and a normal tissue and also helps to detect pre-cancerous cells.

Pharmaceutical applications: Raman spectroscopy is used in identifying pharmaceutical contents and in drug distribution monitoring.

Material characterization: It is useful in nanotechnology in not only identifying but also to knowing the characteristics of nanomaterials and nanoparticles.

Environmental applications: Raman is used to keep track of the amount of the toxins and pollutants present in water [45].

The advancement of Raman spectroscopy and its increasing range of applications has highlighted constraints in traditional methods of spectral data analysis. Consequently, there is emphasis on

exploring innovative approaches to enhance Raman spectroscopy and its analytical techniques within research endeavors. Overall, it is still an effective technique to find out about the molecular structure and behavior of different materials [43].

1.6.3 Fourier Transform Infrared Spectroscopy (FTIR)

FTIR not only helps in identification of the functional group but also helps in identifying the possible bond present in a molecule. The adsorption bands in IR region help in identifying the chemical components that might not have been seen in XPS. Typically, an FTIR spectra lies in the region of $4000\text{-}650\text{ cm}^{-1}$. The frequencies correspond to the vibrational bands of the functional group thus if a frequency is absorbed that particular functional group is present.

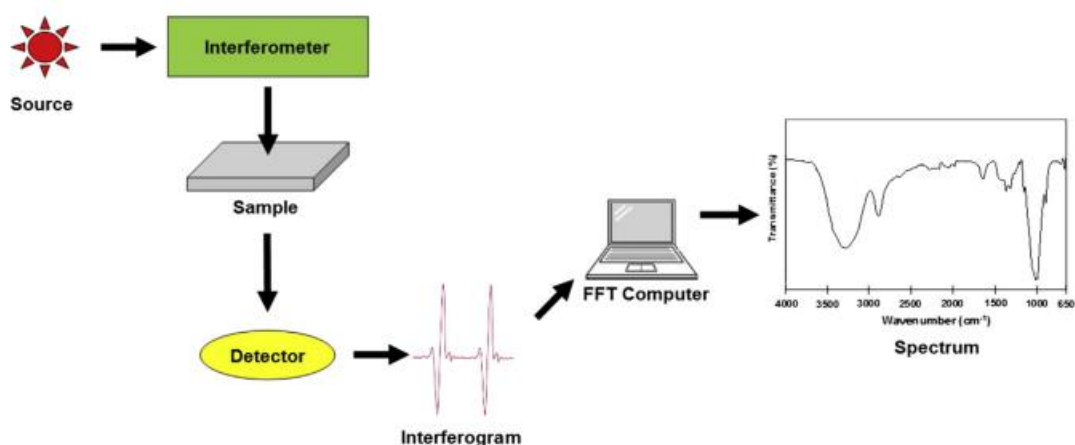


Figure 5 FTIR instrumentation

A beam of electron is emitted by a black body which passes through an interferometer. The electron beam of light is split inside an interferometer. There split electron beams having different path lengths then recombine which gives raise to destructive and constructive

interferences. This is said to be an interferogram. The beam then passes through the sample. Here specific frequencies are absorbed by the samples. These frequencies depend upon the characteristics of the sample therefore are unique for each sample. The beam finally reaches the detector where a superimposed beam is also provided as a reference. The spectrum is then made by subtracting the two beams [46].

1.6.4 Scanning electron microscopy (SEM)

This method gives details of the morphology, structure at microscopic level and about the chemical composition of a compound [47]. SEM is usually paired up with electron disruptive spectroscopy (EDS) to help get the qualitative and quantitative analysis of the sample. Without EDS only the surface structure, morphology, can be studied. SEM consists of an electron gun, a column, scan coils, electron detector, a chamber and a computer system.

First a high energy electron beam is produced from the gun around 100-30,000 eV. Usually, a thermal source produces electron beam. The electron beam is wide therefore it is then passed through a lens to be focused on the sample to generate a focused image. The width of the beam on interaction with the specimen is about 10nm and it goes to a depth of $1\mu\text{m}$.

The beam is moved around the surface of the material by the scan coil. The beam makes lines on the surface to produce a rectangular raster on the surface. The distance between the lens and surface affects the magnification of the image.

The electron detector then detects the electron emitted by the scanned surface. To create the image SEM uses not only secondary electrons (SE) but also backscattered electrons (BSE). The collector screen might collect positive voltage or negative voltage. The positive voltage has both E and BSE in it while the negative voltage has only BSE in it.

The signal is displayed on screen and the operator will control the intensity and brightness to produce a clear image. The signals gathered at each place are used to create the final image as the beam advances line by line in a raster pattern.

Variation in electron accelerating voltage impacts the level of details captured in the scanned image. Lower accelerating voltages have surface information, while higher voltages penetrate deeper, therefore giving information about sample's interior.

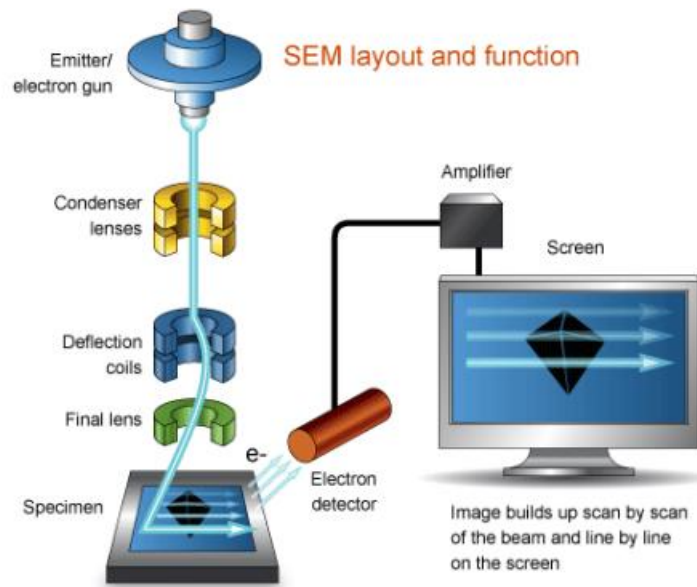


Figure 6 Scanning Electron Microscopy instrumentation

The resulting image provides partly 3D information. The image depends on the topography of the sample and is also effected by the number of BSE and SE. Additionally, the angle at which the sample surface inclines at, usually angles between 50 to 70 degrees, enhance BSE and SE signals, contributing to increased topographic contrast [48].

1.6.5 Transmission electron microscopy (TEM)

It helps in characterization of a material and is one of the powerful techniques present. It especially plays an important role in nanotechnology field. TEM has been used by scientists to look into small particles. Conventionally it has been used in imaging, analysis of chemicals and diffraction of the material [49]. TEM focuses an electron beam on the sample and this interaction between the light and the material forms an image with high resolution that provides information about crystal structure, its size, and composition.

Electron gun produces a beam of electron. There are two types: field emission and thermionic guns. In thermionic emission gun that is more common, there is a cathode that is the source of electron a Wehnelt cylinder grid, and an anode with a central opening.

The electrons are emitted from cathode when high voltage is applied. These electrons have high velocity and energy therefore, Wehnelt cylinder is used which is made negative by the DC current. This reduces the coverage of the electrons beam.

After this electromagnetic lens direct the electron beam on the sample. Four lens are used due to their different properties. These are: Condenser, Objective, Intermediate and Projector lenses. All these provide different functions to the TEM instrument.

Another main component is the vacuum pump, this is necessary so that the electron travels a longer distance without deviating or without interacting with other species that might be present in between the electron gun and the sample.

The last step in TEM is the creation of images. It uses electrons to make the image of the sample, The electrons interact in various ways with the sample such as reflection, diffraction, absorption etc when these electrons finally reach the detector or screen an image is created by converting the electron intensity into visible light.

There are several electron detectors and depending on the requirement a suitable detector can be selected. In conventional TEM, the static incident beam allows easy focusing on the screen, resulting in a fixed analog image that cannot be manipulated during detection. The viewing screen plays a vital role, influencing potential changes in the image.

Depending on where the electrons are physically present the cathodoluminescence (CL) works to present electrons. The emission of light spots on the screen corresponds to the intensity of one or more electrons striking it. The thickness, composition, and the structure of the sample can be predicted by the pattern obtained [50].

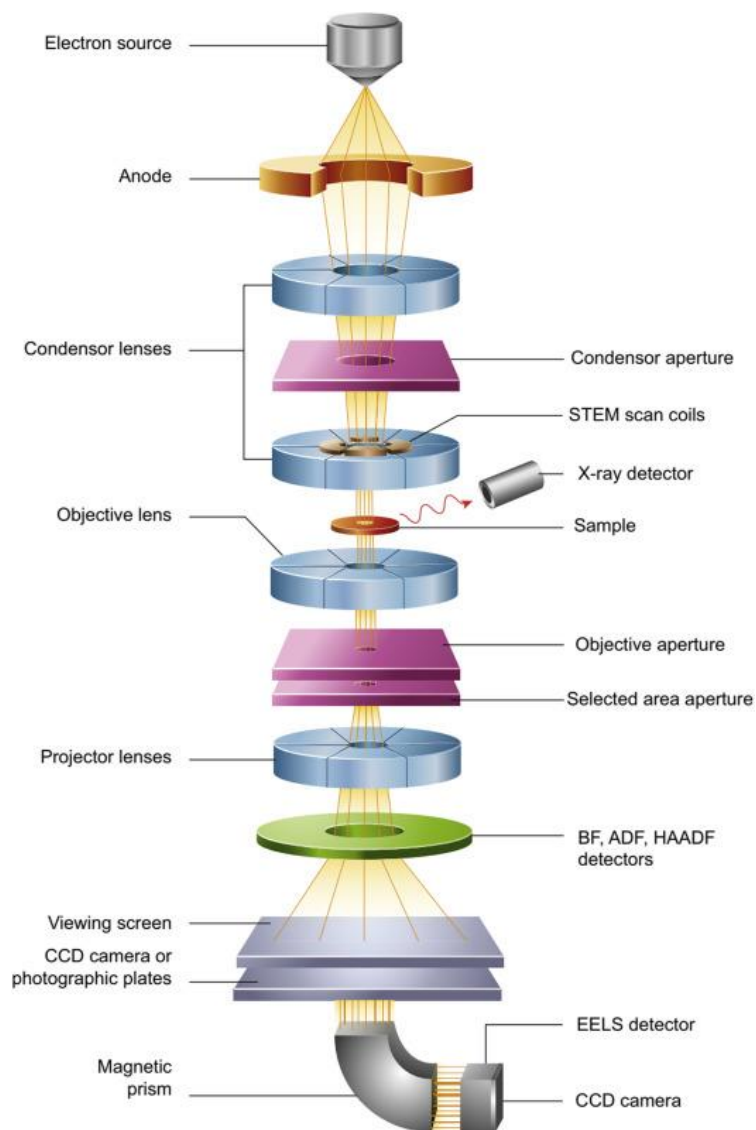


Figure 7 Transmittance Electron Microscopy instrumentation

Apart from nanotechnology TEM has also found wide use in biology. It helps in determining the structure, interaction and the processes that occur at cell level [51]. It has also been used in material sciences to help with the identification of composition and with imaging. Overall, it is a useful technique that has been widely used across different fields.

Chapter 2

1.7 Literature Review

One of the catalyst commonly used in electrochemistry are transition metal phosphides because of multi-active sites present in them and their controllable/tunable composition and structure. Cobalt specifically has been widely used in OER and HER compared to iron and nickel. CoP effectively catalyzes HER and its activity is further enhanced by combining with other TMPs due to the synergic interaction between CoP and other TMP. In this study *CoP₂/CoP* heterojunction structure was used which exhibited an overpotential of 196mV at 10mAcm^{-2} for HER and Tafel slope of 53 mV dec^{-1} . *CoP₂/CoP* was synthesized through one-step calcination. Two different quantities of $\text{CoCl}_2 \cdot 6\text{H}_2\text{O}$ were taken to synthesize CoP and *CoP₂*. $\text{CoCl}_2 \cdot 6\text{H}_2\text{O}$ was placed with $\text{NaH}_2\text{PO}_2 \cdot \text{H}_2\text{O}$ at the ends of boat and the temperature was increased for 2 h to 400 celcius in presence of argon at $2\text{ }^\circ\text{C min}^{-1}$. After that it was with distilled H_2O and $\text{C}_2\text{H}_5\text{OH}$ and then dried for 12 hours at about $70\text{ }^\circ\text{C}$ [52].

An alternate fuel conversion method is low temperature fuel cells due to their cleanness and inexhaustible energy. In fuel cells ORR acts as cathode and the electrocatalysts used for this is Pt for higher selectivity and activity. Cobalt phosphide nanorods provide a cheaper and efficient alternate and therefore were used for ORR in alkaline solution. *CoP₂* was synthesized through reflux, $\text{Co}(\text{Ac})_2$, TOPO, and OLAC were dissolved in benzyl ether in a flask with tree neck. It was

then degassed, and nitrogen was filled in it. Reaction temperature was then set at 200 °C and TBP was added after which it continued for 60 min at 260 °C. It was then washed with toluene and acetone after cooling and centrifuged at 7000rpm. Finally, CoP_2NRs were collected and redispersed in hexane [53].

Hydrogen has been accepted as an alternate energy source to fossil fuel and therefore designing an efficient and cost-effective catalyst is crucial. Here Cobalt phosphide-anchored N-doped carbon is synthesized through pyrolysis. For this a solution was made in DI water of $Co(NO_3)_2 \cdot 6H_2O$, $C_2H_5NO_2$ and phytic acid. The solution was then dried resulting in $Co/P@NC$. This was pyrolyzed at 900 °C under N_2 environment and 3 hours to form product. The product with $Co:P=1:0.89$, showed elevate HER activity and stability. It gave about 202 mV overpotential when density was 10 mA cm^{-2} [54].

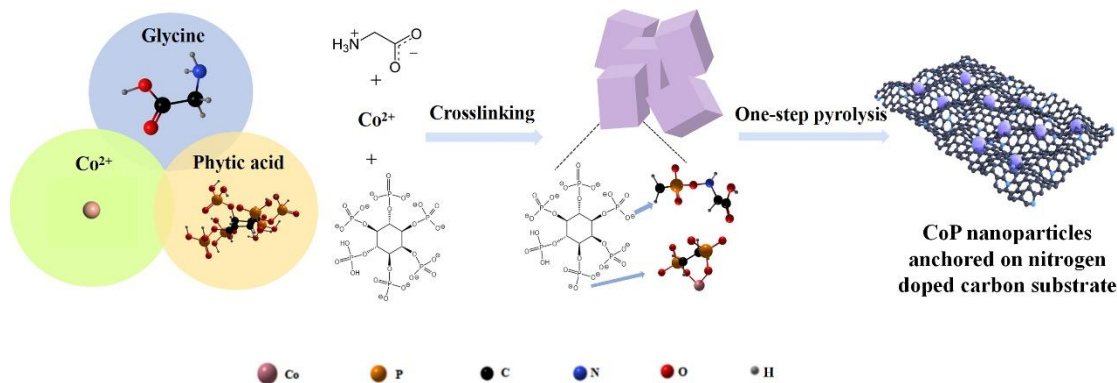


Figure 8 Synthesis of $CoP@N$ doped C

Supercapacitors as emerged as a device favorable for storing energy due to their higher rates of charging/discharging, power density and environmental friendliness with longer lifetime. Ordered

carbon mesoporous (OMCs) has been used as electrode material as it elevates specific surface areas and has large pores with tunable structure. But it has an inherently low energy density thus hinders its application therefore TMPs are considered as effective material for supercapacitors. Among these Cobalt Phosphide provides high capacitance through faradic reactions. Herein porous cobalt phosphide nanoflakes on OMC was synthesized by phosphidating the hydrothermally synthesized Co@OMC to be used as a bifunctional material for HER and ESC. OMC prevents agglomeration and also provides a $413.4 \text{ m}^2 \text{ g}^{-1}$ surface area to CoP. For synthesis a solution was made in water of NH_4F , $\text{CO}(\text{NH}_2)_2$ and $\text{Co}(\text{NO}_3)_2 \cdot 6 \text{H}_2\text{O}$ and OMC. A homogeneous mixture of this was poured in autoclave and it was set at $120 \text{ }^\circ\text{C}$ for 5 h. Purple precipitant, of Co@OMC, formed were washed and were dried. The precursor with $\text{NaH}_2\text{PO}_2 \cdot \text{H}_2\text{O}$ were placed in furnace and annealed for 2h at $300 \text{ }^\circ\text{C}$ at $5 \text{ }^\circ\text{C min}^{-1}$ rate and in N_2 environment. The product gained is CoP@OMC. The product showed 3182 Fg^{-1} specific capacity at current density 1 A g^{-1} . Moreover, it showed an overpotential of 111mV for HER [55].

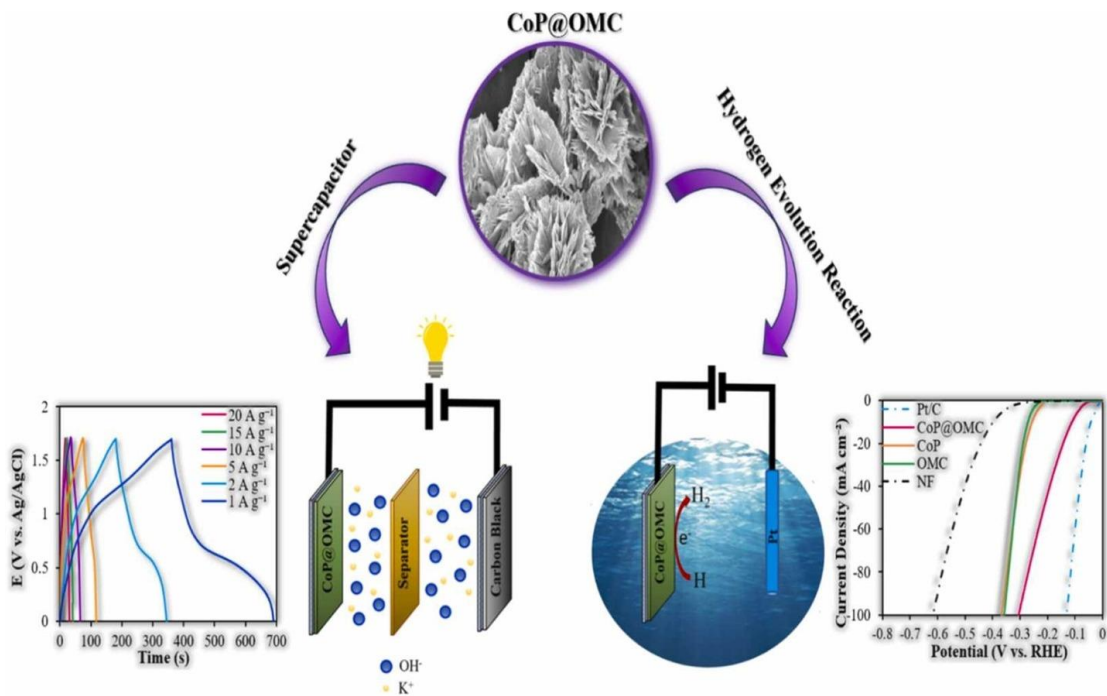


Figure 9 CoP@OMC used as bifunctional material for HER and ESC

In another study, cobalt phosphide was synthesized using microwave-assisted hydrothermal method. For this, a solution was made in DI water containing $\text{CoCl}_2 \cdot 6\text{H}_2\text{O}$ and cetyltrimethyl ammonium bromide (CTAB) which was transferred to a digestion vessel where it was made airtight with yellow phosphorus. It was then heated to 220°C for 30 mins using microwave digestive system. The solution color turned black and precipitates of Co_2P were separated by centrifugation. The synthesized Co_2P nanoshuttles showed outstanding specific capacity of 246 F/g at current density 1 A/g and great cycling ability, indicating that it can be used for energy storage or energy conversion [56].

Co_3P is comparatively less studied for HER as an electrocatalyst. Though has a distinct electronic properties and structural feature due to polyphosphide present and can facilitate proton reduction.

In this study the Co_3P was synthesized by first depositing $CoCl_2$ on carbon from methanol solution and then it is dried. $CoCl_2/C$ was reacted with red phosphorous at $500^\circ C$. Co_3P gave density of about 10 mA cm^{-2} when a potential of -95 mV was applied to it [57].

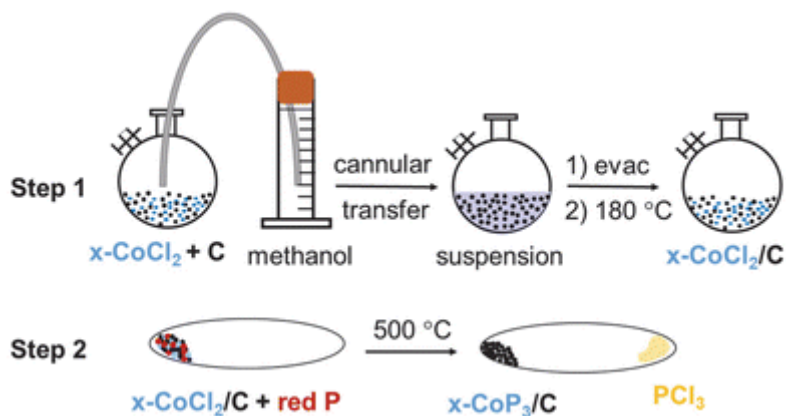


Figure 10 Synthesis of Co_3P using red phosphorous

In this study hyperbranched Co_2P nanocrystals were synthesized through a new method that were uniform in shape, size and symmetry. In this $Co(Ac)_2$ was decomposed in TOPO at $350^\circ C$ in air free atmosphere. Co_2P nanoparticles were formed and the formation was confirmed by XRD, SEM and TEM [58].

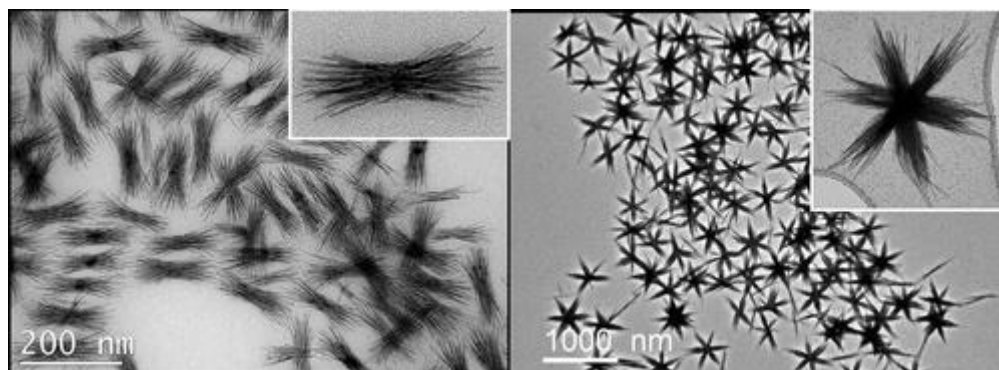


Figure 11 Structure of hyperbranched Co₂P nanocrystals

Aniline is important for synthesis of several chemicals like dyes, pharmaceuticals, pigments and agrochemicals. Reduction of nitro group is one of the most important and easy methods to manufacture anilines. Therefore, designing a selective catalyst that would selectively reduce nitro group in without reducing other groups is pivotal. In this study Co₃O₄-NGr@C, is made through pyrolysis of amino-ligand cobalt acetate. The catalyst was used to convert nitroarenes to aniline through transfer hydrogenation. For this reaction 20mg f catalyst, 1mmol of nitrobenzene, 3.5mmol of formic acid, as a source of H₂ was taken along with THF and Et₃N. It was observed that Co(OAc)₂-Phen/C pyrolyzed at 800°C for 2 hours gave a yield of 96% and conversion of 99% [59].

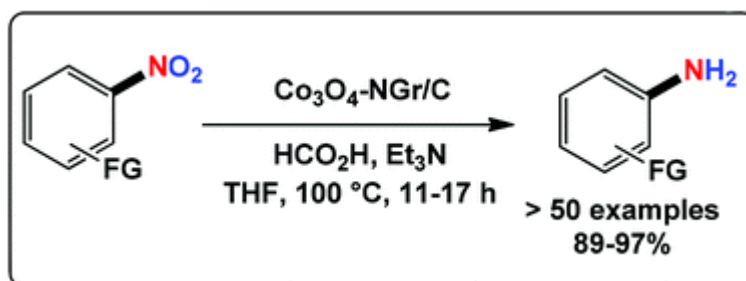


Figure 12 Reduction of nitroarenes to aniline

Metal-organic frameworks (MOFs) has been a leading material in research due to its internal surface area, designable topologies and pores. Therefore, in this study $\text{Co}_2\text{P}/\text{CN}_x$ nanocubes are synthesized using MOFs. Uniform cubes of ZIF-67 were first synthesized using cetyltrimethylammonium bromide which were then mixed with red phosphorus and calcinated to form $\text{Co}_2\text{P}/\text{CN}_x$ nanocubes. These cubes of cobalt phosphide after characterization using XRD, XPS and TEM were used for hydrogenation of different nitroarenes substrates. They showed a selectivity and conversion of 99% for most of the substrates at 50MPa and 60°C in 6hours. The TEM results discovered that Co_2P was made at high temperatures of 700-900°C. Whereas SEM showed the uniform distribution of Co_2P particles on the nanocubes formed [23].

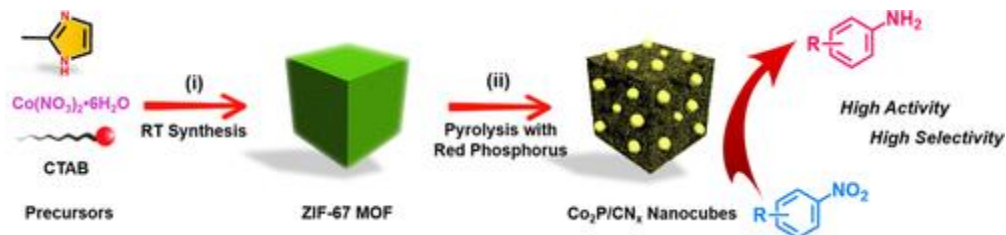


Figure 13 Synthesize of Cobalt phosphide using ZIF-67 and red phosphorus

Chemoselective reduction of nitroarenes is a significantly desirable reactions in pharmaceutical, pesticide and chemical industry. In this study stable, renewable and reusable cobalt particles on carbon are synthesized and used for hydrogenation. Here carbon-supported cobalt particles are synthesized using macroalgae to make them highly dispersed. 50 mg of the catalyst was used in THF/H₂O to carry out hydrogenation in a high-pressure autoclave. At 40 bar and 120°C for 18 hours, the catalyst that was calcinated at 800°C was able to give a 99% conversion with 99% selectivity. Cobalt particles formation was confirmed by using XRD, XPS, Raman and TEM [60].

Thermal decomposition of ZIF-67 in N₂ atmosphere can be used to synthesize cobalt nanoparticles on nitrogen doped carbon (Co@NC). This is an excellent catalyst for the reduction of anilines which play a large role in industries. This is a recyclable, scalable and active heterocatalyst unlike many catalysts that suffer from difficult recyclization and separation from product. Co@NC calcinated at 800°C was able to give 99% conversion of nitrobenzene to aniline at 30 bar and 110°C [61].

In this study the single atom cobalt on nitrogen doped graphene (Co@N_x-C) is synthesized from acrylonitrile. Co@N_x-C annealed at 800°C hydrogenated nitroarenes to aniline. At 120°C and 15 bar the catalyst showed excellent selectivity and conversion of approximately 99%. Cobalt chloride hexahydrate and acrylonitrile were reflux in ethyl acetate and AIBN to form blue precipitates. The precipitates were mixed with colloidal-SiO₂ to form a solution and from it the solvent was removed to get dark green precipitates which was annealed at different temperatures

then treated with HF to get Co@Nx-C. Further research is still being done on SACs to hydrogenate nitroarenes at milder conditions [62].

Herein cobalt particles on carbon with a nanosheet structure are synthesized in solvothermal conditions. For this furfural, acting as carbon source and $\text{Co}(\text{AC})_2 \cdot 4\text{H}_2\text{O}$, was used as a cobalt source. Both were mixed with H_2O and ethyl glycol and were kept in autoclave for 15 h at $180\text{ }^\circ\text{C}$ to form precipitates. The precipitates were calcinated at different temperatures $300\text{-}900\text{ }^\circ\text{C}$ for 3 hours at $2\text{ }^\circ\text{C}/\text{min}$ under nitrogen atmosphere to form Co/C catalyst. The catalyst showed 98% conversion and 97% selectivity towards chloronitrobenzene at $140\text{ }^\circ\text{C}$ and 20 bar for 3 h [63].

Chapter 3

1.8 Methodology

1.8.1 Cobalt-TPP synthesis

To synthesize cobalt phosphide first a cobalt-TPP complex was synthesized through a solvothermal method. 0.4g of Cobalt chloride hexahydrate ($\text{CoCl}_2 \cdot 6\text{H}_2\text{O}$) was dissolved in acetic acid. In a separate beaker 1.5g of triphenylphosphine (TPP) was dissolved in 20ml of acetic acid. The two solutions were mixed, and the color changed to blue. It was then stirred for 2 hours at 30°C and was later filtered to separate the blue precipitates formed. These were then washed with acetic acid.

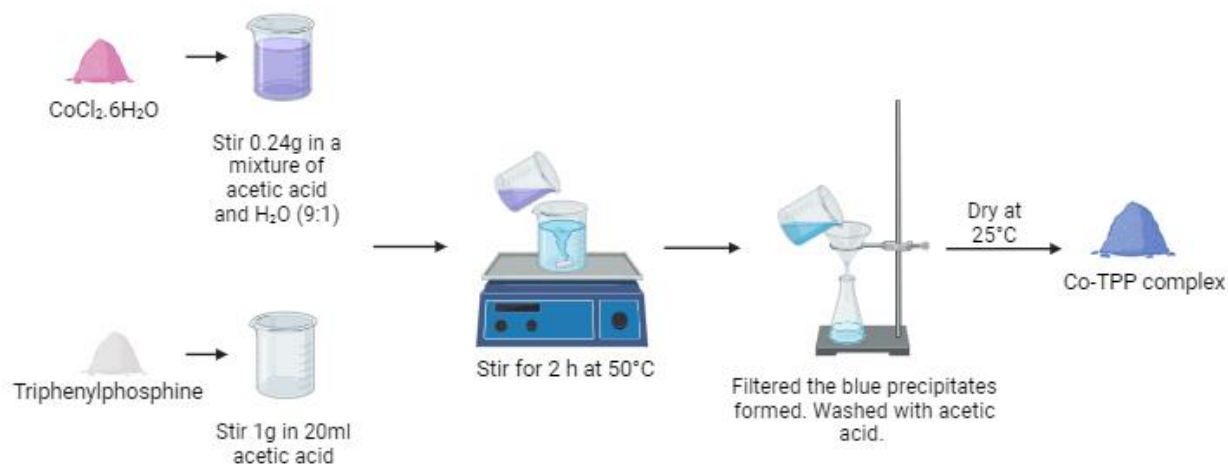


Figure 14 Schematic diagram for Co-TPP complex synthesis

1.8.2 Cobalt-TPP deposition on AC

In the second step the deposition of complex on activated carbon (AC) was carried out. For this the precipitates were dissolved in chloroform and 0.8g of activated carbon was added. Chloroform was left to evaporate with constant stirring to homogenously deposit the complex on the activated carbon. The black solid obtained was then left at 60°C to dry.

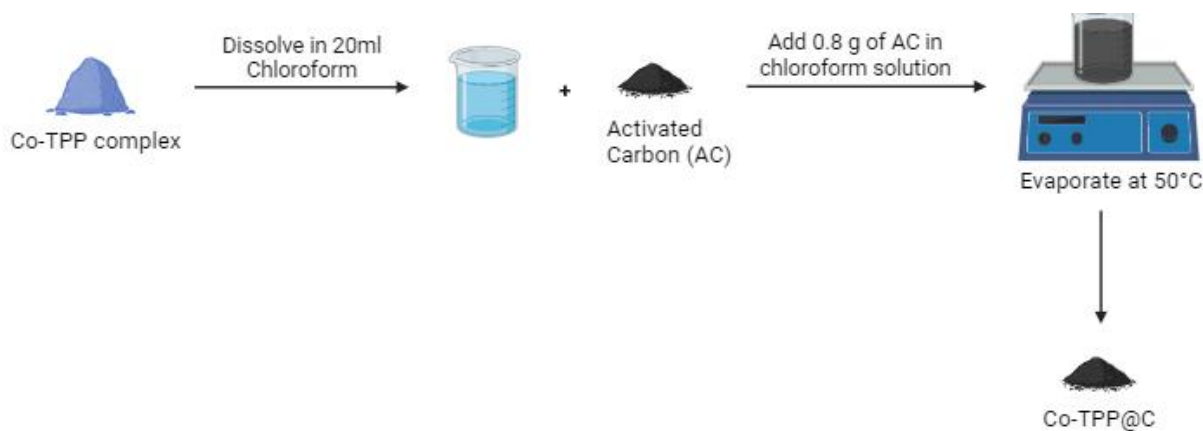


Figure 15 Schematic diagram for deposition of Co-TPP complex on activated carbon

1.8.3 Decomposition of Cobalt-TPP complex

The black solid obtained in step 2 was calcinated for 2h at three temperatures 400°C, 600°C and lastly 800°C with a ramp time 5°C/min to compare activity. Black powder was formed as a result of calcination which was then further characterized and used in application.



Figure 16 Pyrolysis of complex to gain Co_2P/C

1.9 Chemical Equation

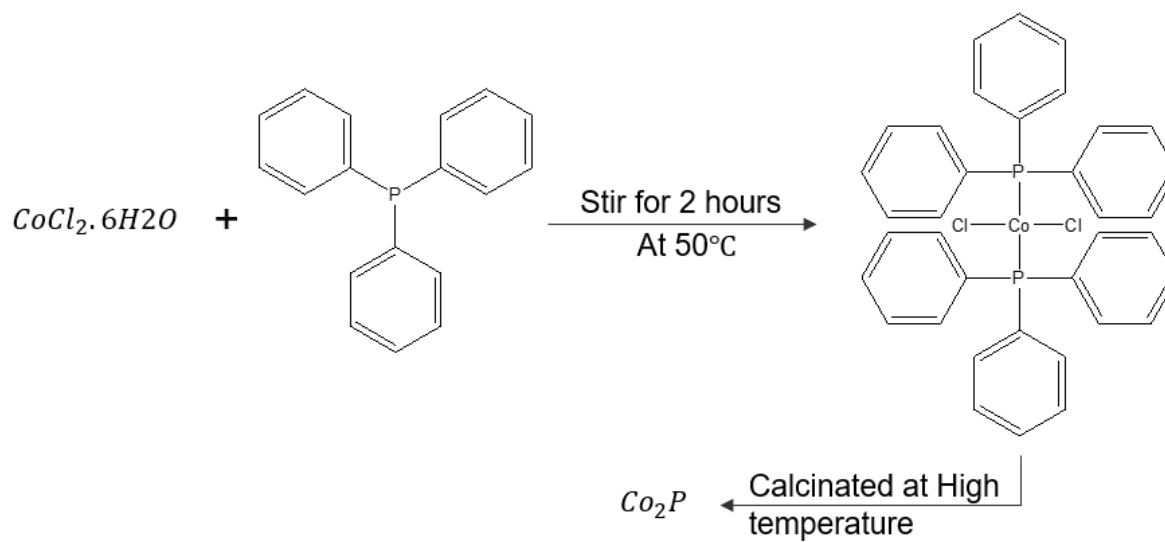


Figure 17 Proposed reaction for the synthesis of Co_2P

Chapter 4

1.10 Characterization

1.10.1 X-Ray Diffraction

The obtained cobalt phosphide sample was identified pXRD. The peaks observed at 2θ values of 40.7° , 43.3° , 48.3° , 50.3° and 56.2° correspond to [121], [211], [031], [310] and [320] planes of orthorhombic phase Co_2P (JCPDs # 32-0306). At 26.6° and 28.5° peaks corresponds to activated carbon [64].

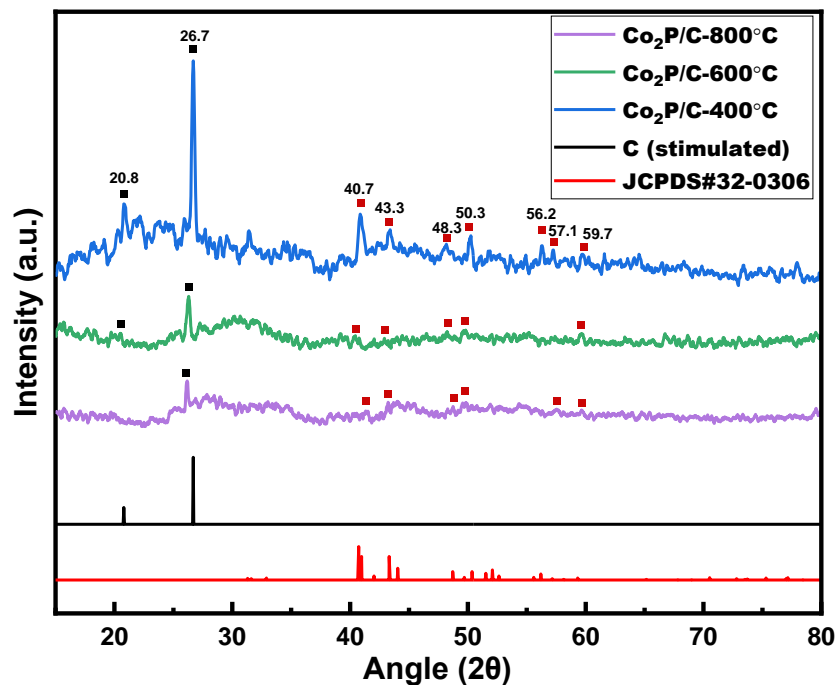


Figure 18 pXRD spectrum of Co₂P/C@800, Co₂P/C@600 and Co₂P/C@400

1.10.2 Raman Spectroscopy

The Raman peaks at 228 and 303 cm^{-1} attribute to Co-P bond [65]. The peaks at 1333 and 1588 cm^{-1} are D-band, hybridization sp^3 , and G-band, hybridization sp^3 , of the amorphous carbon present [66]. The peak at 1088 cm^{-1} represents sp^3 vibrations for H-free carbon and it appears only in UV-Raman [67].

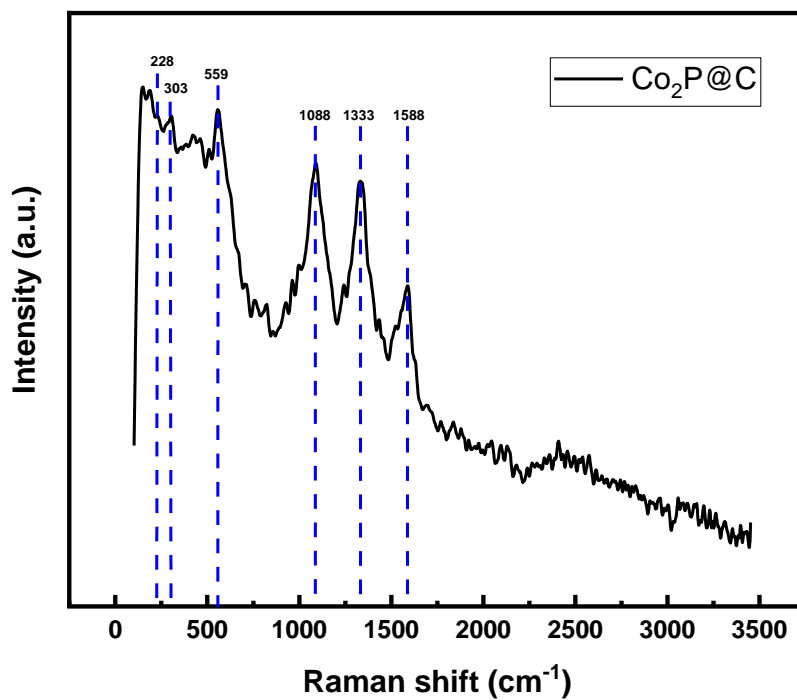


Figure 19 Spectra of Co₂P/C@800

1.10.3 Fourier-Transform Infrared Spectroscopy (FTIR)

The peaks around 1000 cm^{-1} and 1200-1600 cm^{-1} is assigned to CoP [68].

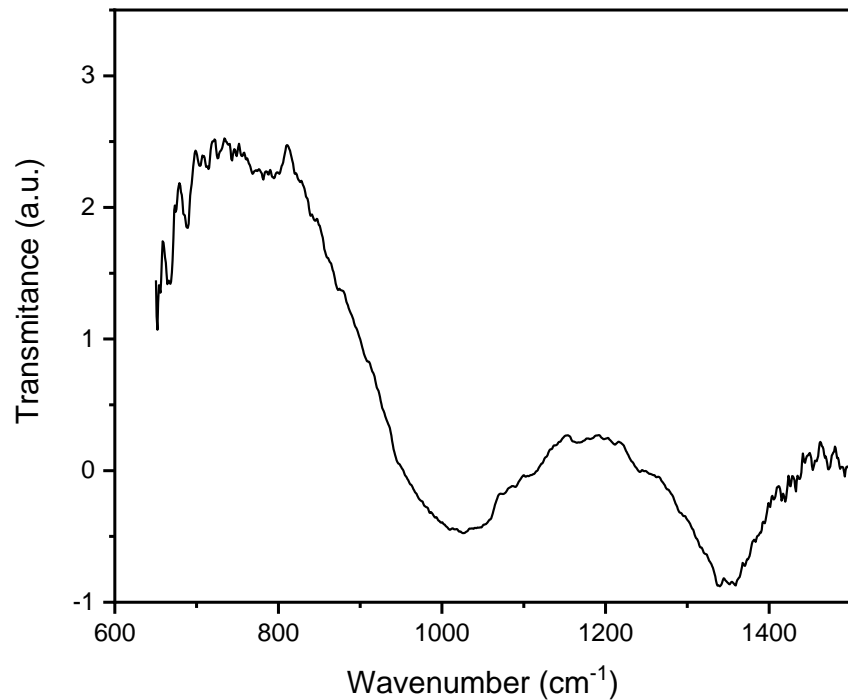


Figure 20 FTIR of Co₂P/C@800

1.10.4 Scanning Electron Microscopy

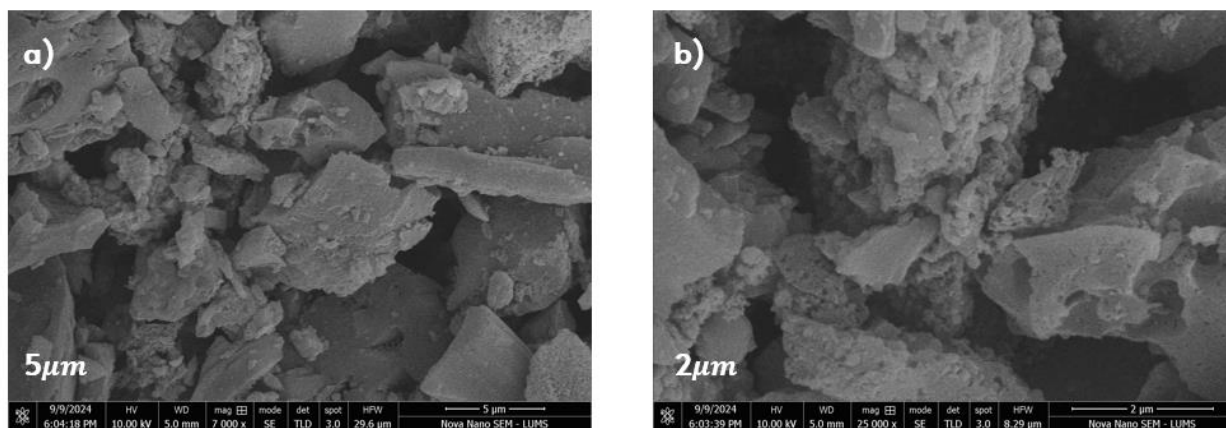


Figure 21 Scanning electron microscopy image of Co₂P/C@800 at a) 5 μm and b) 2 μm

1.10.5 Energy Disruptive X-ray analysis

The energy dispersive X-ray spectroscopy of Co₂P/C@800 depicts that Co, P are uniformly distributed over carbon layer surface. The wt.% of C, O, Co and P came out to be 74.94, 12.43, 6.78, and 2.44% respectively.

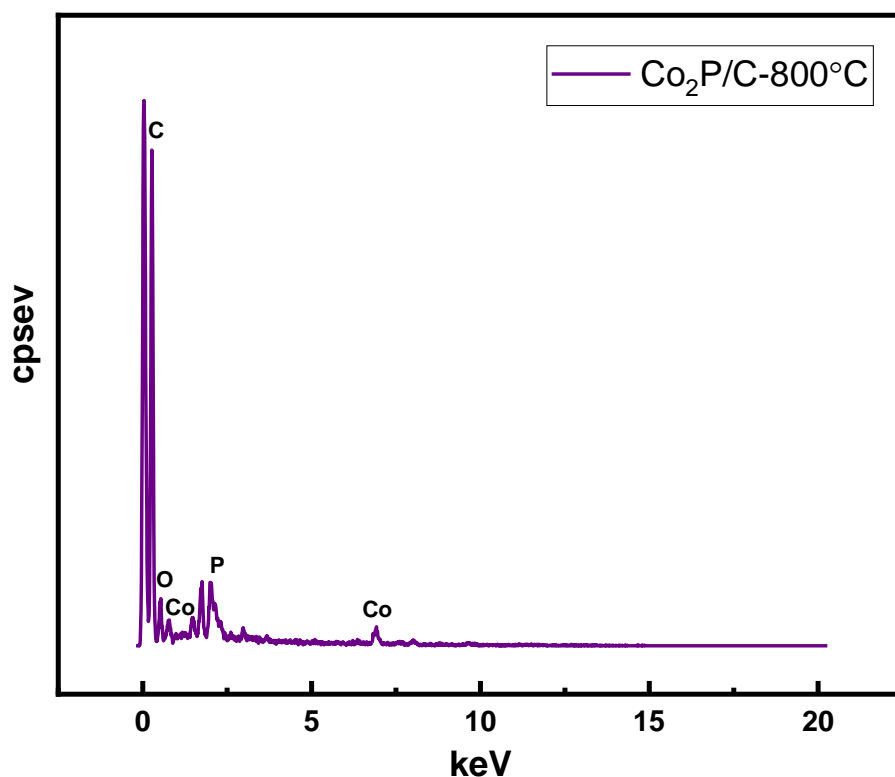


Figure 22 EDS spectrum of Co₂P/C@800

1.10.6 Transmission Electron Microscopy

The TEM analysis of synthesized Co₂P/C@800 catalyst has given an in-depth analysis of its morphology. TEM images Exhibits that Co₂P is well distributed and immersed in porous carbon

layers. Moreover the inter planar distances of 0.338 and 0.418 nm are in accordance with the 002 plane of C and 0.222 nm corresponds to the 121 plane of Co_2P .

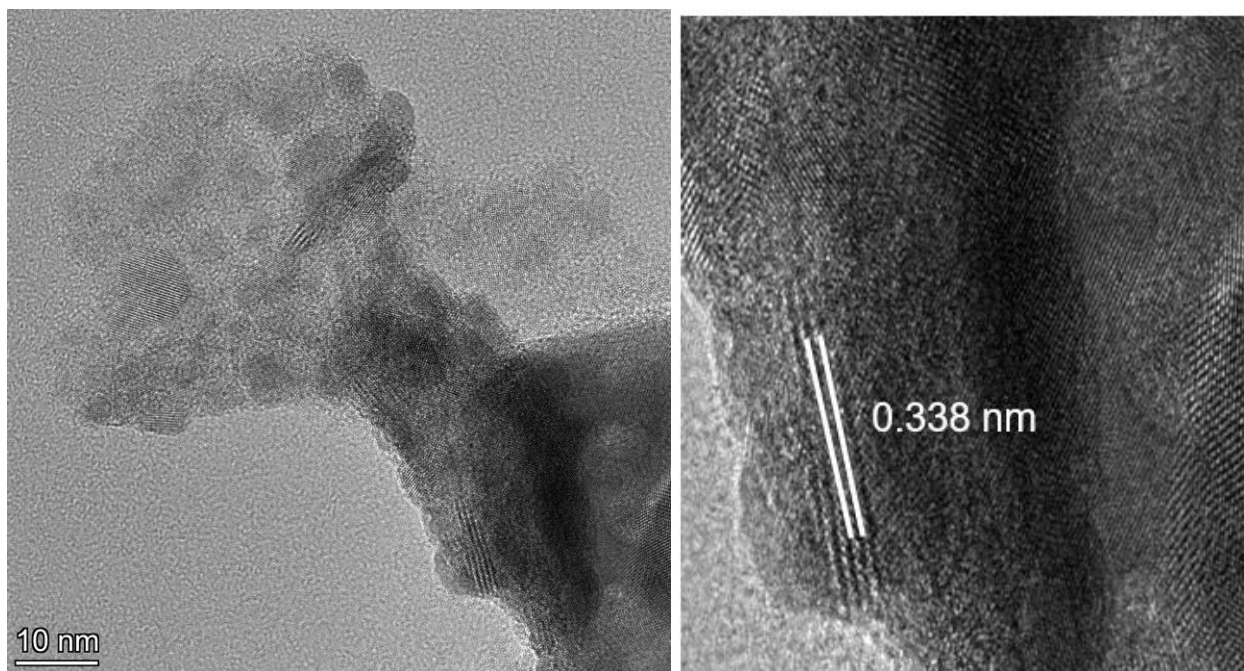


Figure 23 TEM image of $\text{Co}_2\text{P}/\text{C}@800$ at 10nm

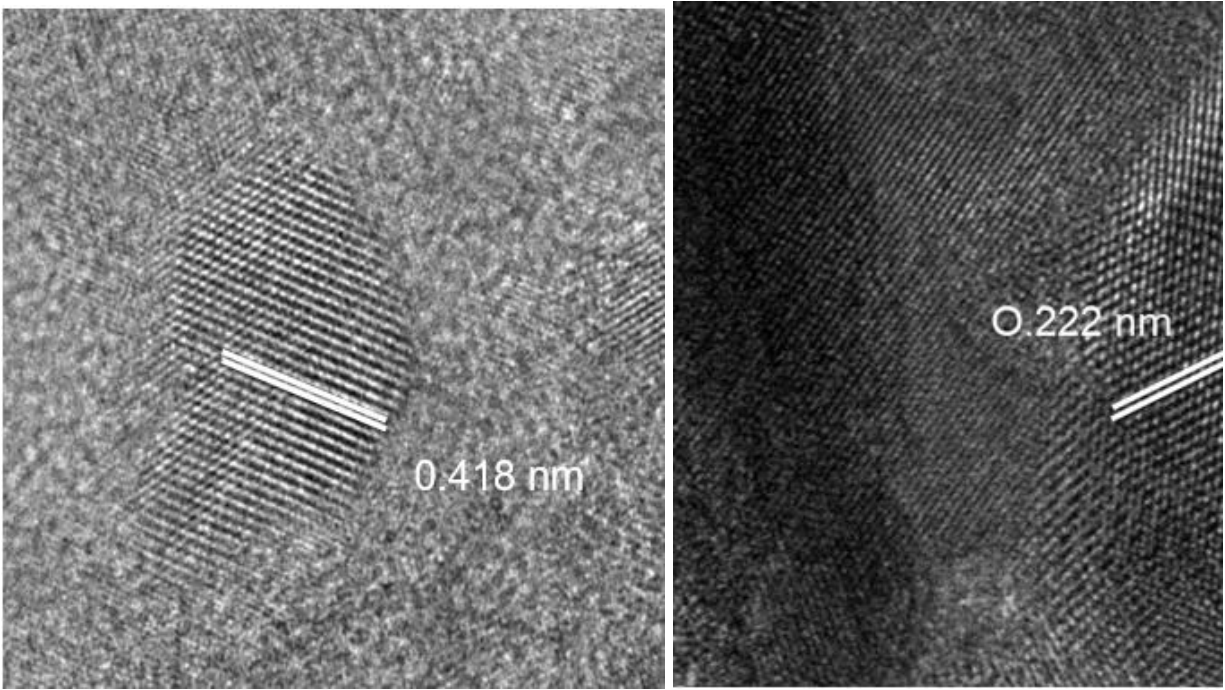


Figure 24 HRTEM image of Co₂P/C@800at 10nm

1.11 Application

The reduction reaction was done in a high-pressure autoclave. To carry this out a solution was made of $2\mu\text{L}$ or 2mg of substrate in 4 ml of methanol in a vial. To this a specific amount of catalyst was added along with the stirrer and syringe was placed in it. The vial was then placed in the high-pressure autoclave which was then sealed and was flushed twice with H_2 . Then H_2 gas was filled to get a defined pressure. The autoclave was then placed in the hot plate. The temperature was then set at $120\text{ }^\circ\text{C}$ for 20 hours. The product formed was filtered and then analyzed through Gas Chromatogram-Mass Spectrophotometer.

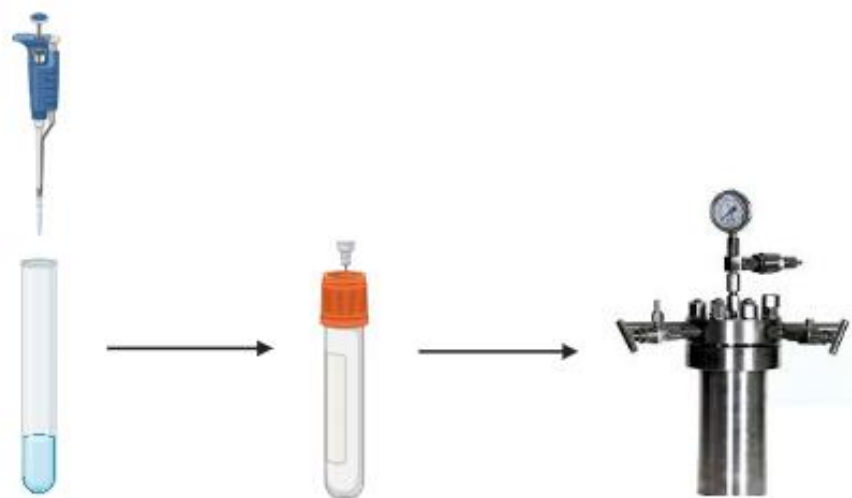
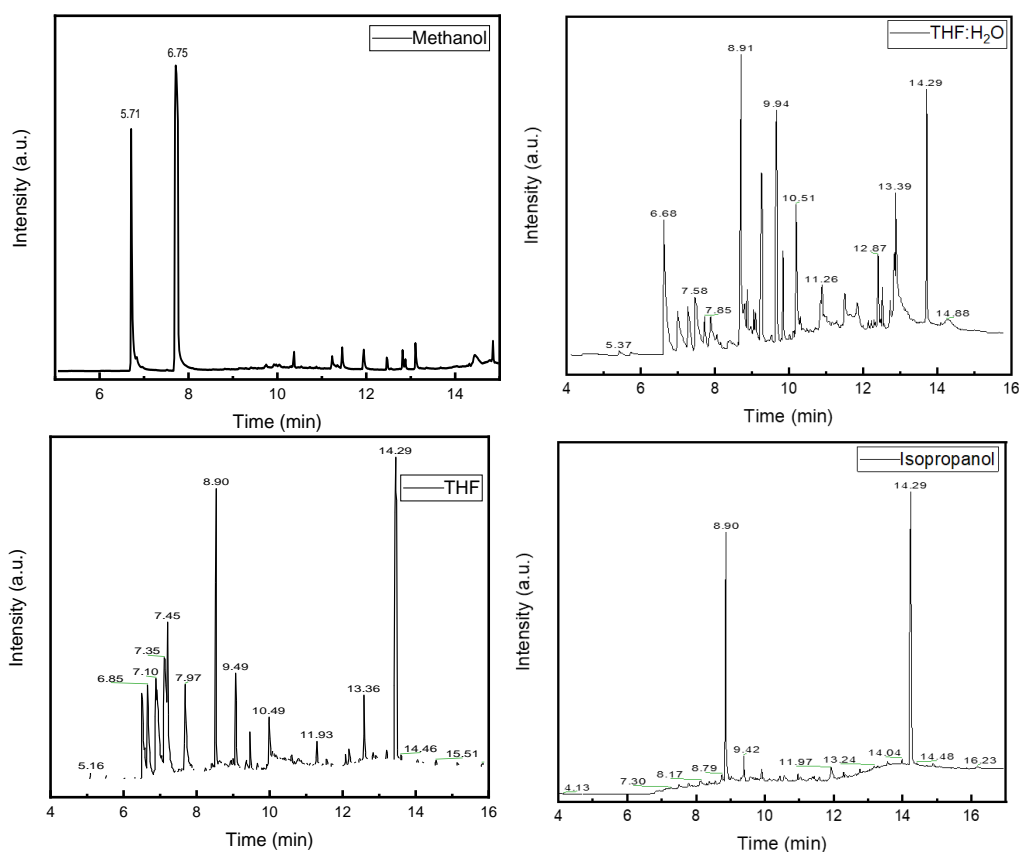


Figure 25 Schematic diagram for nitroarene molecular hydrogenation

1.11.1 Optimization reactions using catalytic reduction of nitrobenzene

The selective reduction of nitrobenzene was carried out at different pressures and solvents using 25mg of the catalyst, keeping the temperature at 120°C for 0 hours. Four different solvents are used. Out of this methanol showed 100% selectivity while THF, THF:H₂O and isopropanol give 0% selectivity. Therefore for rest of the reactions methanol was used.



At 15 bar the selectivity of nitrobenzene reduction was 99% but the conversion of only 20% as interpreted from the GC-MS spectra. The retention time of 6.75 is of nitrobenzene and 5.72 is of

aniline. Similarly at 25 bar, selectivity of nitrobenzene reduction was 99% and a conversion 90% was achieved.

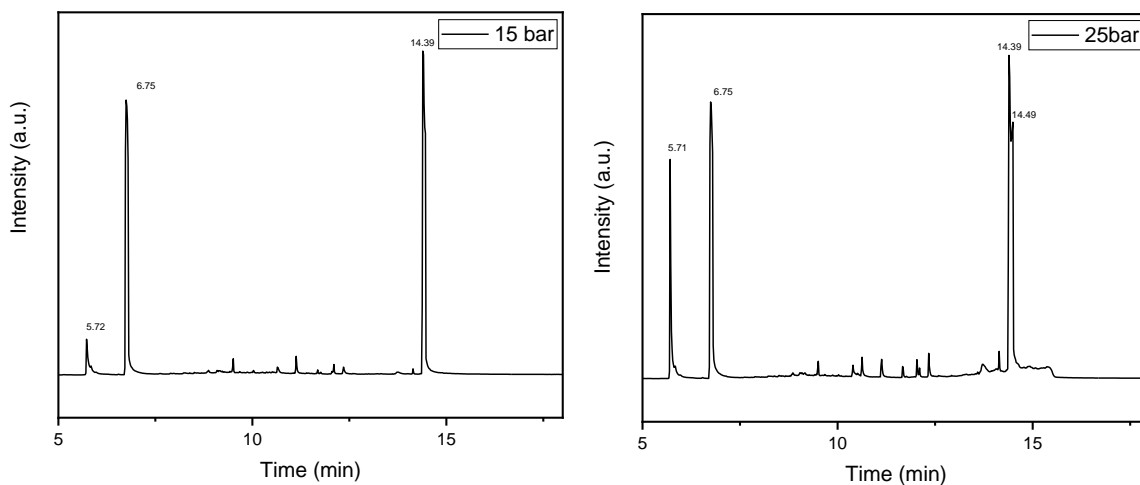


Figure 26 Gas Chromatogram of Aniline at a) 15 bar and b) at 25 bar

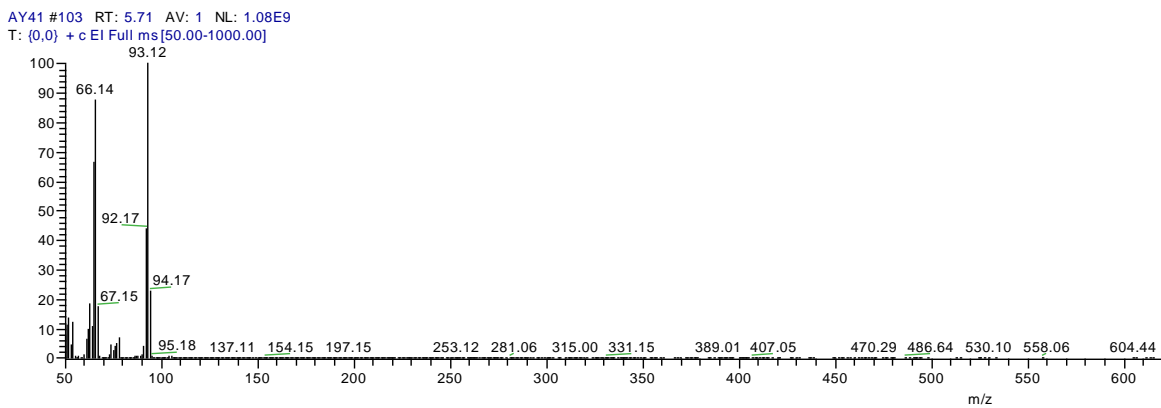
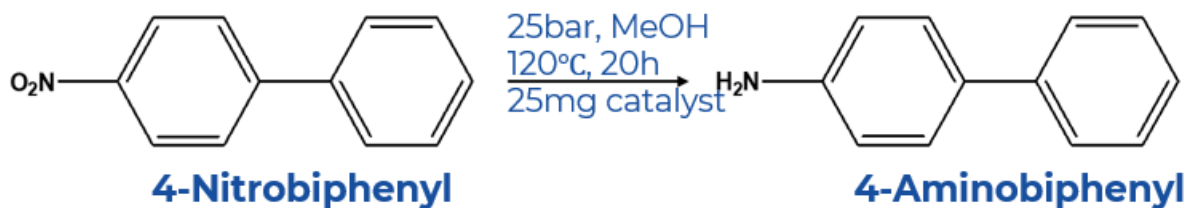


Figure 27 MS spectra of Aniline

1.11.2 Catalytic reduction of p-Nitrobiphenyl



The selective reduction p-Nitrobiphenyl was also carried out at two different pressures using 25mg of the catalyst, keeping the temperature at 120°C for 0 hours. At 20 bar the selectivity of p-Nitrobiphenyl reduction was 99% and the conversion of about 87-90% as interpreted from the GC-MS spectra. The retention time of 11.58 is of p-Aminobenzene and 12.32 is of p-Nitrobenzene. At 30 bar, selectivity was 0% and a conversion of 100% was achieved.

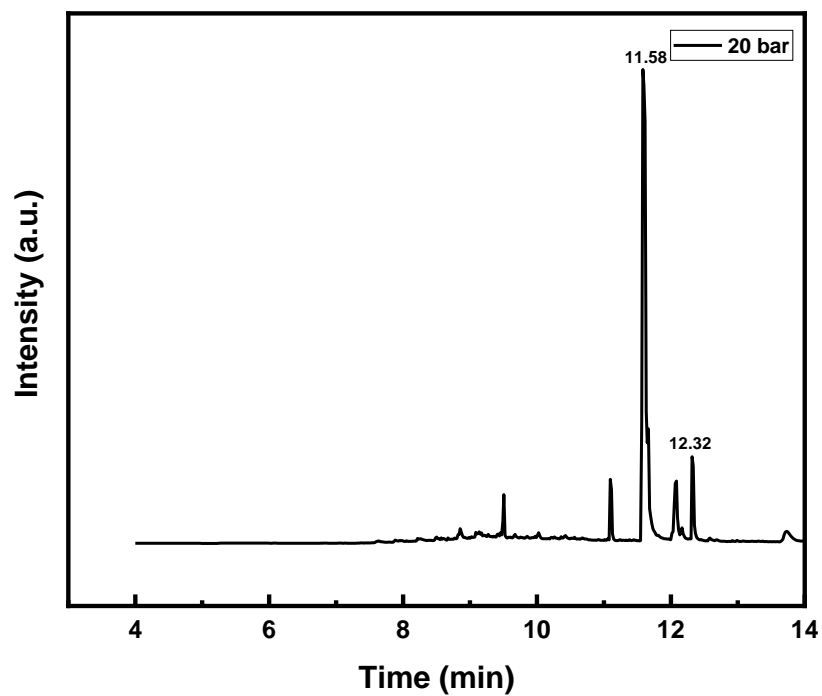


Figure 28 Gas Chromatograph of *p*-Aminobiphenyl

AY57 #454 RT: 11.58 AV: 1 NL: 1.03E9

T: {0,0} + c EI Full ms[50.00-1000.00]

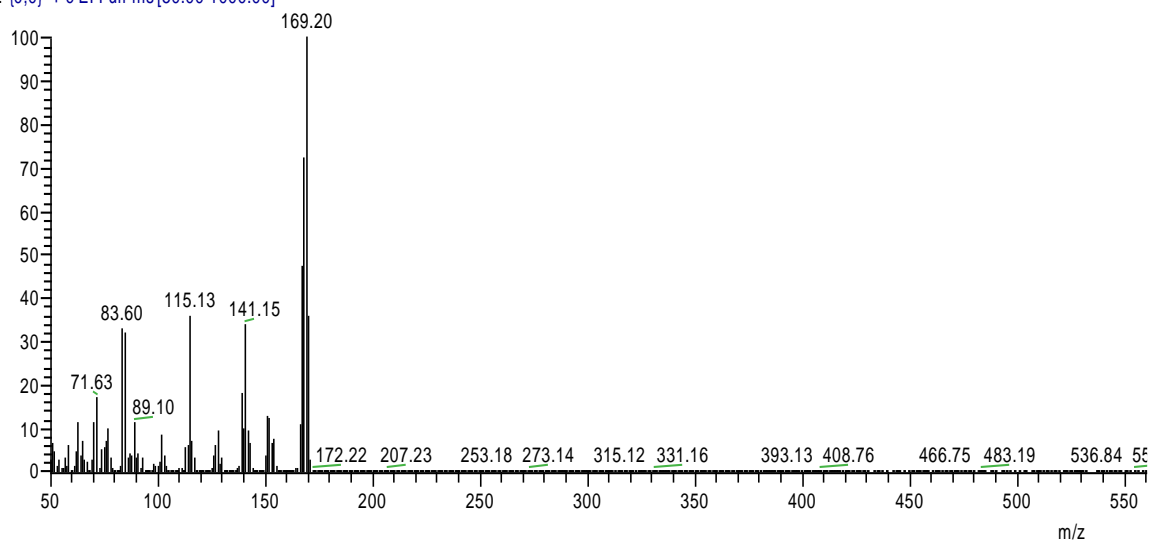
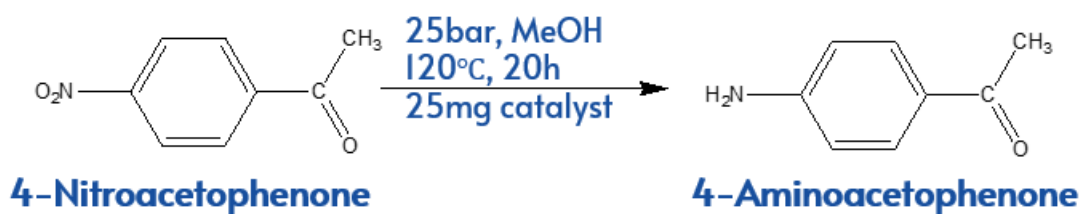


Figure 29 MS spectra of *p*-Aminobiphenyl

1.11.3 Catalytic reduction of different substrates at 25 bar:

After optimizing different substrates reduced at 25bar keeping rest of the parameters same.

1.11.3.1 Catalytic reduction of 4-Nitroacetophenone:



4-Nitroacetophenone is reduced into 4-Aminoacetophenone at a pressure of 25 bar and temperature of 120 °C with 25 mg catalytic amount for 20 hours. 100 % conversion of 4-Nitroacetophenone occurred with 99% selectivity.

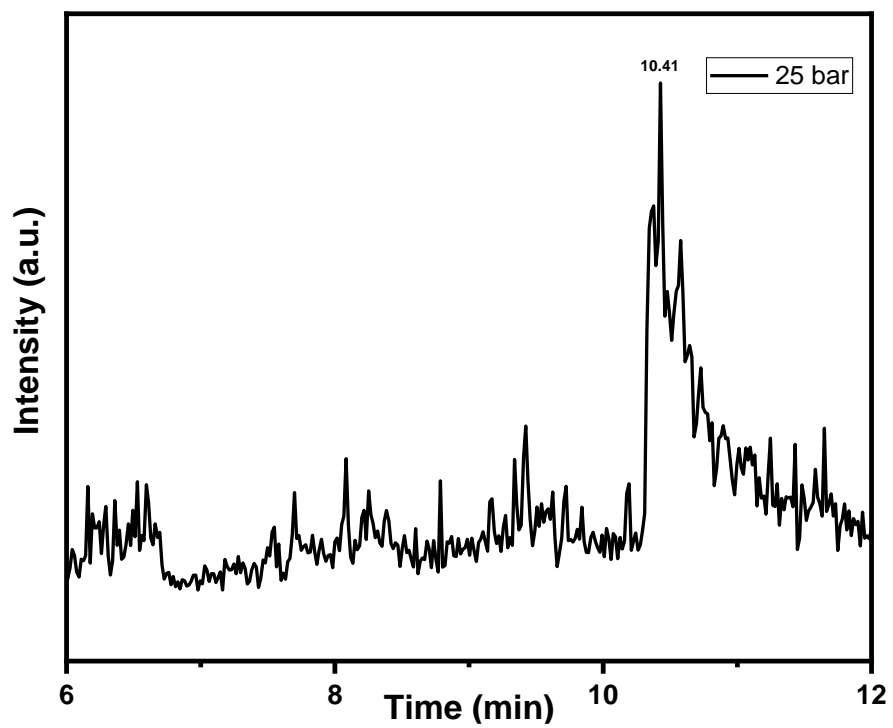


Figure 30 Gas Chromatogram of 4-Aminoacetophenone at 25 bar

S-1 #384 RT: 10.41 AV: 1 NL: 5.16E4
T: {0,0} + c EI Full ms [50.00-1000.00]

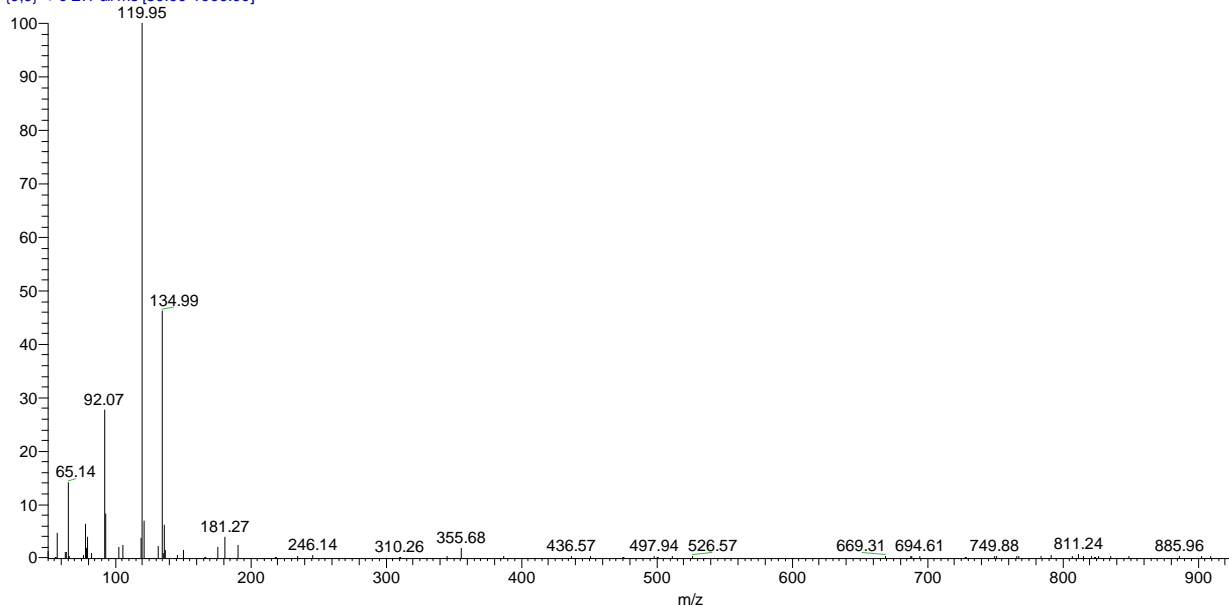
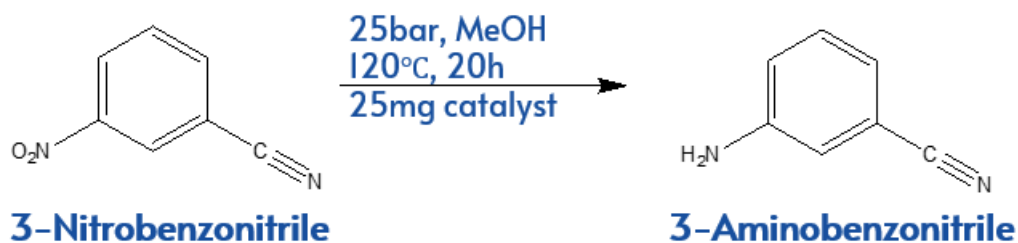


Figure 31 MS spectra of 4-Aminoacetophenone

1.11.3.2 Catalytic reduction of 3-Nitrobenzonitrile:



Nitrobenzonitrile is reduced into Aminobenzonitrile at a pressure of 25 bar and temperature of 120 °C with 25 mg catalytic amount for 20 hours. 100 % conversion of Nitrobenzonitrile occurred with 99% selectivity.

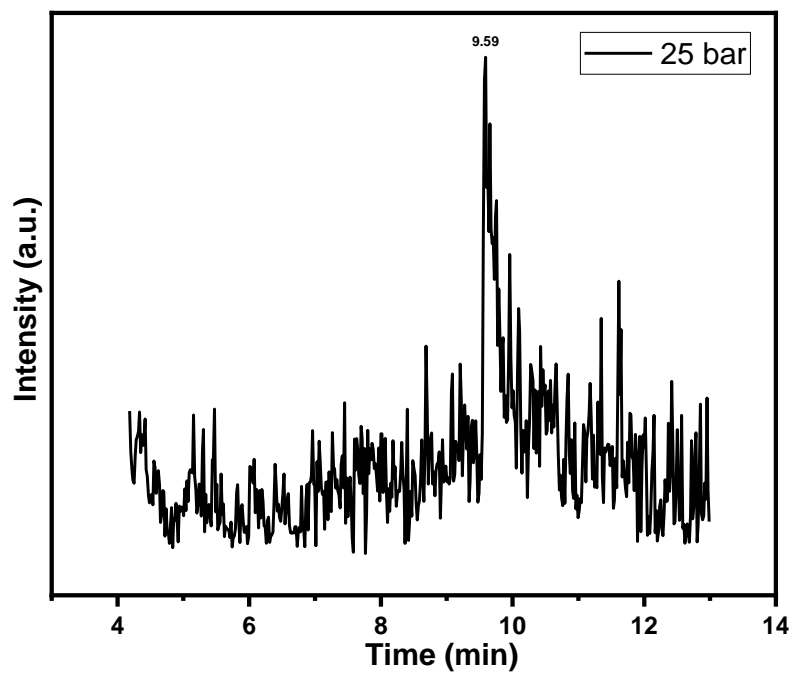


Figure 32 Gas Chromatogram of 3-Aminobenzonitrile at 25bar

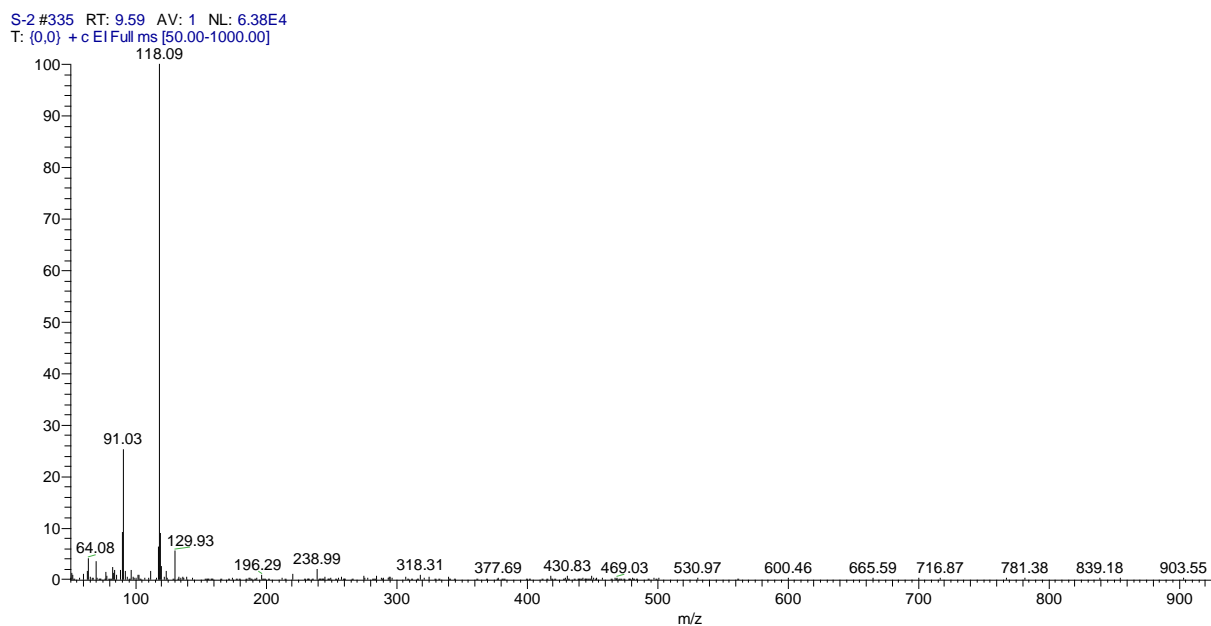
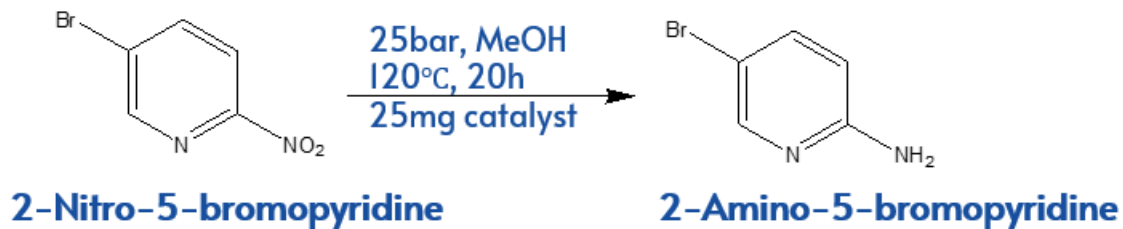


Figure 33 MS spectra of 3-Aminobenzonitrile

1.11.3.3 Catalytic reduction of 2-Nitro-5-bromopyridine:



2-Nitro-5-bromopyridine is reduced into 2-Amino-5-bromopyridine at a pressure of 25 bar and temperature of 120 °C with 25 mg catalytic amount for 20 hours. 100 % conversion of 2-Nitro-5-bromopyridine occurred with 99% selectivity.

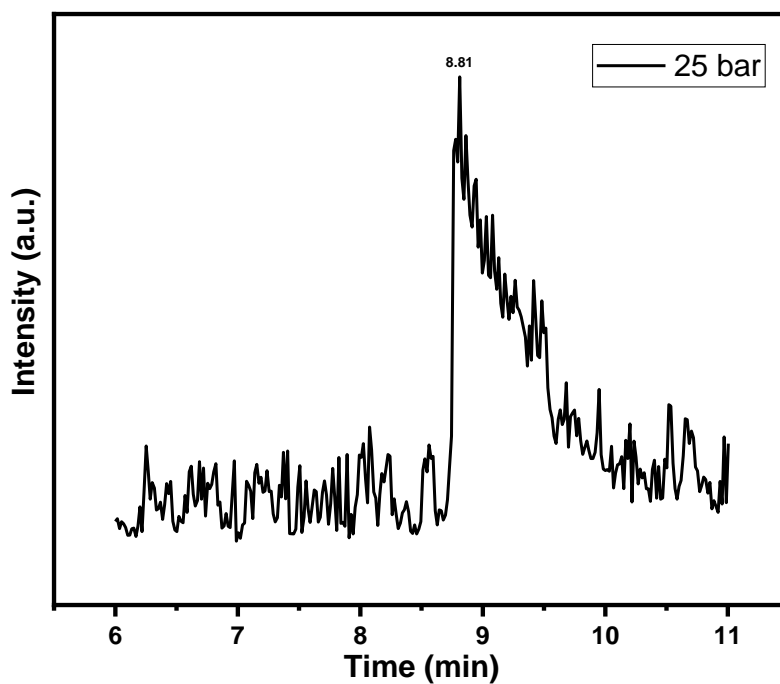


Figure 34 Gas Chromatogram of 2-Amino-5-bromopyridine at 25bar

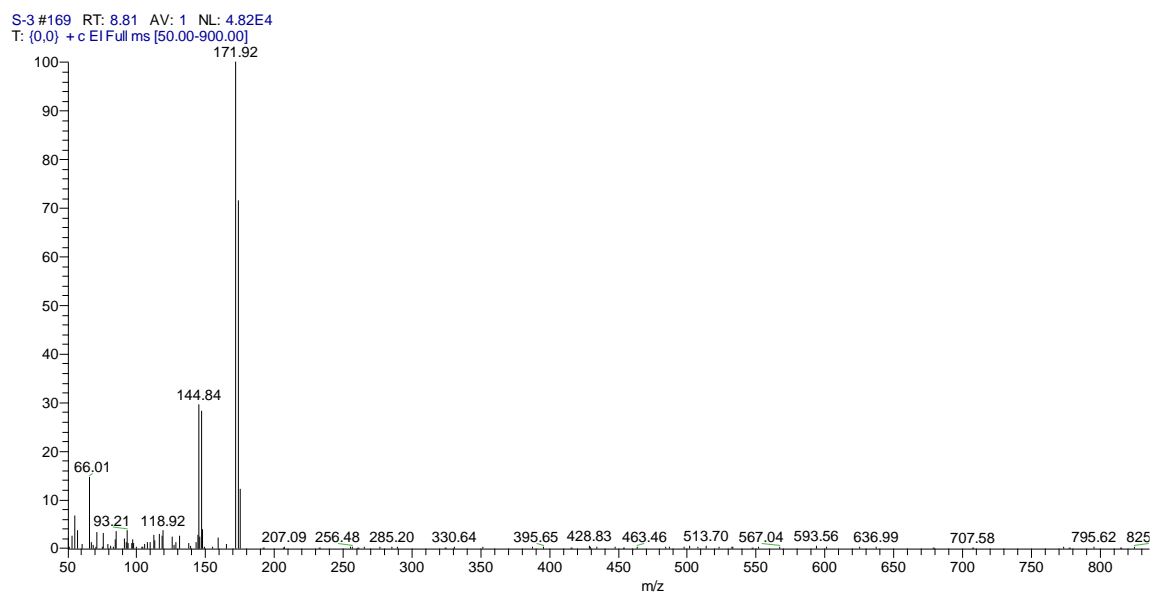
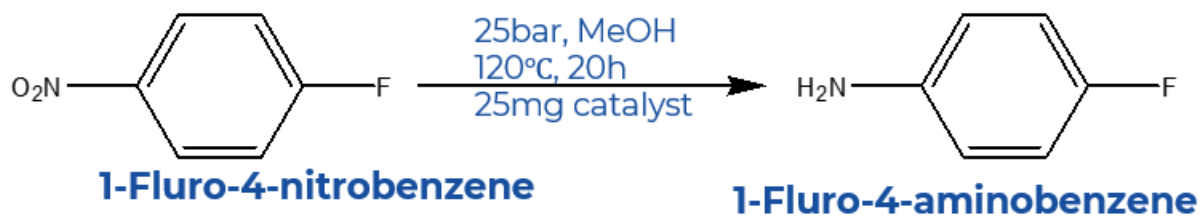


Figure 35 MS spectra of 2-Amino-5-bromopyridine

1.11.3.4 Catalytic reduction of 1-Fluoro-4-nitrobenzene:



1-Fluoro-4-nitrobenzene is reduced into 1-Fluoro-4-aminobenzene at a pressure of 25 bar and temperature of 120 °C with 25 mg catalytic amount for 20 hours. 100 % conversion of 1-Fluoro-4-nitrobenzene occurred with 99% selectivity.

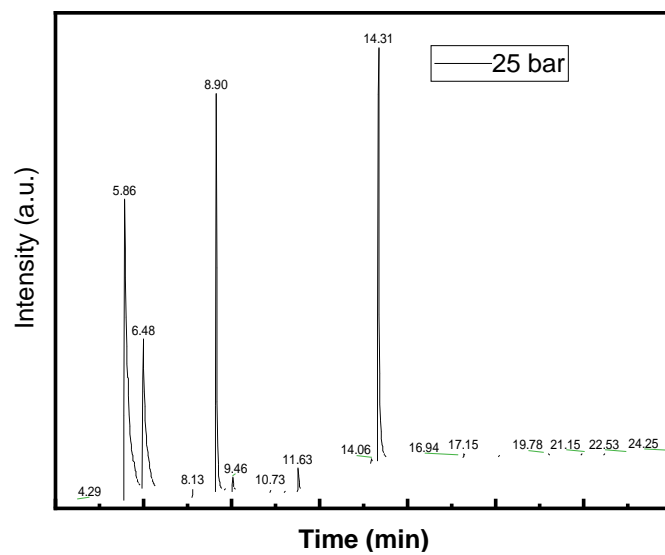


Figure 36 Gas Chromatogram of 1-Fluoro-4-aminobenzene

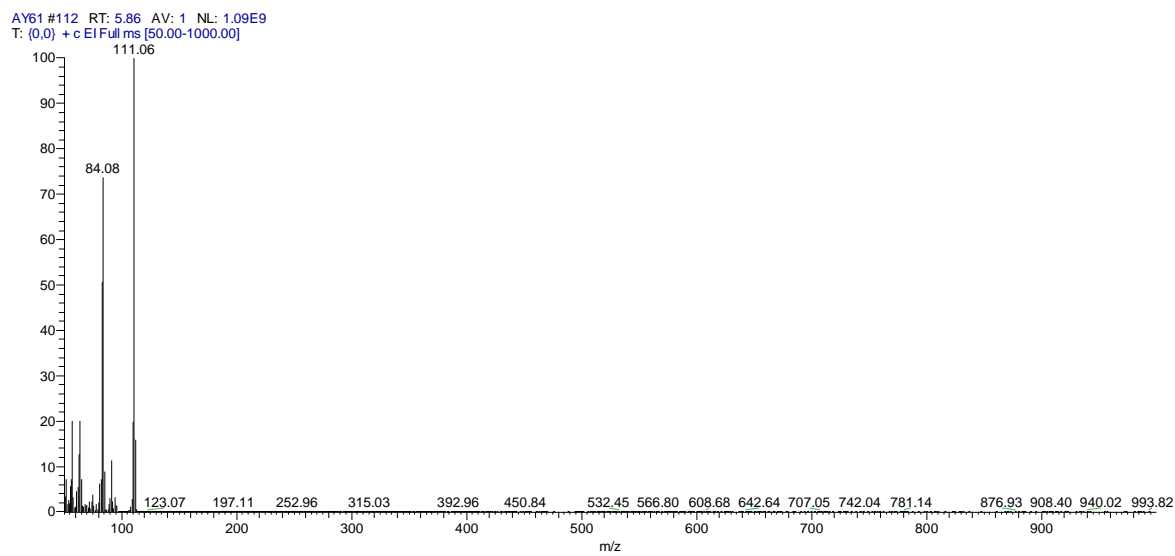
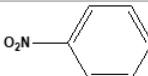
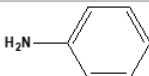
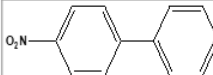
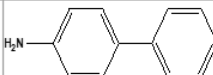
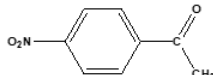
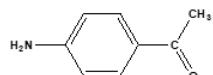
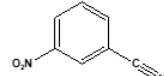
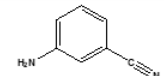
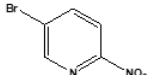
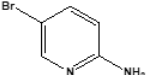
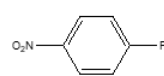
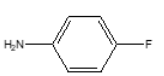


Figure 37 MS spectra of 1-Fluoro-4-aminobenzene

Substrate	Product	Pressure	Conversion%	Selectivity%
		25 bar	45	>99
		20 bar	87-90	>97
		25 bar	100	>99
		25 bar	100	>99
		25 bar	100	>99
		25 bar	75	>99

Conclusion

Co₂P/C was synthesized using a salt of cobalt and triphenylphosphine as a source of phosphorous through an easy, environment friendly and cost-effective method. This method is safe as it avoids the production of phosphine gas which is usually produced in other methods where different phosphorous sources are used. The synthesized Co₂P/C@800 exhibited high catalytic activity converting 100% of 3-Nitrobenzonitrile, 4-Nitroacetophenone and 2-Nitro5-bromopyridine to their amine analogues at 25bar. It showed an 87% conversion of p-Nitrobiphenyl to p-Aminobiphenyl at 20 bar. And a 60% conversion of Nitrobenzene at 25 bar. In all these nearly >99% selectivity was achieved.

References

1. Fechete, I., Y. Wang, and J.C. Védrine, *The past, present and future of heterogeneous catalysis*. Catalysis Today, 2012. **189**(1): p. 2-27.
2. Friend, C.M. and B. Xu, *Heterogeneous catalysis: a central science for a sustainable future*. Accounts of chemical research, 2017. **50**(3): p. 517-521.
3. Hu, X. and A.C. Yip, *Heterogeneous catalysis: enabling a sustainable future*. 2021, Frontiers Media SA. p. 667675.
4. Fujita, S., et al., *Ni₂P Nanoalloy as an Air-Stable and Versatile Hydrogenation Catalyst in Water: P-Alloying Strategy for Designing Smart Catalysts*. Chemistry–A European Journal, 2021. **27**(13): p. 4439-4446.
5. Ariga, K. and M. Shionoya, *Nanoarchitectonics for coordination asymmetry and related chemistry*. Bulletin of the Chemical Society of Japan, 2021. **94**(3): p. 839-859.
6. Ishikawa, H., et al., *Air-stable and reusable cobalt phosphide nanoalloy catalyst for selective hydrogenation of furfural derivatives*. ACS Catalysis, 2021. **11**(2): p. 750-757.
7. Callejas, J.F., et al., *Synthesis, characterization, and properties of metal phosphide catalysts for the hydrogen-evolution reaction*. Chemistry of Materials, 2016. **28**(17): p. 6017-6044.
8. Feng, L. and H. Xue, *Advances in transition-metal phosphide applications in electrochemical energy storage and catalysis*. ChemElectroChem, 2017. **4**(1): p. 20-34.
9. Cui, X., et al., *A General Route for Encapsulating Monodispersed Transition Metal Phosphides into Carbon Multi-Chambers toward High-Efficient Lithium-Ion Storage with Underlying Mechanism Exploration*. Advanced Functional Materials, 2023. **33**(15): p. 2212100.
10. Boyanov, S., et al., *Nanostructured transition metal phosphide as negative electrode for lithium-ion batteries*. Ionics, 2008. **14**: p. 183-190.
11. Jin, J. and U. Schwingenschlögl, *Exploration of the two-dimensional transition metal phosphide MoP₂ as anode for Na/K ion batteries*. npj 2D Materials and Applications, 2024. **8**(1): p. 31.

12. Zhang, N., et al., *High-performance flexible solid-state asymmetric supercapacitors based on bimetallic transition metal phosphide nanocrystals*. ACS nano, 2019. **13**(9): p. 10612-10621.
13. Zhi, L., et al., *3D holey hierarchical nanoflowers assembled by cobalt phosphide embedded N-doped carbon nanosheets as bifunctional electrocatalyst for highly efficient overall water splitting*. J. of Colloid and Interface Sci., 2022. **616**: p. 379-388.
14. Zhang, H., et al., *Bifunctional heterostructured transition metal phosphides for efficient electrochemical water splitting*. Advanced functional materials, 2020. **30**(34): p. 2003261.
15. Sun, K., et al., *Incorporating transition-metal phosphides into metal-organic frameworks for enhanced photocatalysis*. Angewandte Chemie, 2020. **132**(50): p. 22937-22943.
16. Yang, Y., et al., *Recent advances in application of transition metal phosphides for photocatalytic hydrogen production*. Chemical Engineering Journal, 2021. **405**: p. 126547.
17. Wei, L., et al., *Recent advances of transition metal based bifunctional electrocatalysts for rechargeable zinc-air batteries*. Journal of Power Sources, 2020. **477**: p. 228696.
18. Yildiz, A., et al., *Efficient iron phosphide catalyst as a counter electrode in dye-sensitized solar cells*. ACS Applied Energy Materials, 2021. **4**(10): p. 10618-10626.
19. Lakshmy, S., et al., *A review of electrochemical glucose sensing based on transition metal phosphides*. Journal of Applied Physics, 2023. **133**(7).
20. Wei, M., et al., *Highly sensitive and selective dopamine sensor uses three-dimensional cobalt phosphide nanowire array*. Journal of Materials Science, 2021. **56**: p. 6401-6410.
21. Wei, P., et al., *Recent advances in chemosensors based on transition metal phosphides for food safety detection*. Trends in Food Science & Technology, 2024: p. 104611.
22. Singsen, S., et al., *Transition-metal decorated graphdiyne monolayer as an efficient sensor toward phosphide (PH₃) and arsine (AsH₃)*. Physical Chemistry Chemical Physics, 2022. **24**(43): p. 26622-26630.
23. Yang, S., et al., *MOF-derived cobalt phosphide/carbon nanocubes for selective hydrogenation of nitroarenes to anilines*. Chemistry—A European Journal, 2018. **24**(17): p. 4234-4238.
24. Shaheen, S., et al., *Recent advances in transition metal phosphide nanocatalysts for H₂ evolution and CO₂ reduction*. Catalysts, 2023. **13**(7): p. 1046.

25. Lawrence, S.A., *Amines: synthesis, properties and applications*. 2004: Cambridge University Press.
26. Murugesan, K., et al., *Catalytic reductive aminations using molecular hydrogen for synthesis of different kinds of amines*. *Chemical Society Reviews*, 2020. **49**(17): p. 6273-6328.
27. Liu, J., et al., *Triphenyl phosphite as the phosphorus source for the scalable and cost-effective production of transition metal phosphides*. *Chemistry of Materials*, 2018. **30**(5): p. 1799-1807.
28. Shi, Y. and B. Zhang, *Recent advances in transition metal phosphide nanomaterials: synthesis and applications in hydrogen evolution reaction*. *Chemical Society Reviews*, 2016. **45**(6): p. 1529-1541.
29. Su, J., et al., *Synthesis and application of transition metal phosphides as electrocatalyst for water splitting*. *Science bulletin*, 2017. **62**(9): p. 633-644.
30. Ni, Y., et al., *Co₂P nanostructures constructed by nanorods: hydrothermal synthesis and applications in the removal of heavy metal ions*. *New Journal of Chemistry*, 2009. **33**(10): p. 2055-2059.
31. Baig, N., I. Kammakam, and W. Falath, *Nanomaterials: A review of synthesis methods, properties, recent progress, and challenges*. *Materials advances*, 2021. **2**(6): p. 1821-1871.
32. Xue, H., et al., *Scalable and energy-efficient synthesis of Co_xP for overall water splitting in alkaline media by high energy ball milling*. *Sustainable Energy & Fuels*, 2020. **4**(4): p. 1723-1729.
33. Lu, Y., et al., *Synthetic methods and electrochemical applications for transition metal phosphide nanomaterials*. *RSC advances*, 2016. **6**(90): p. 87188-87212.
34. Chebrolu, V.T., et al., *The one-step electrodeposition of nickel phosphide for enhanced supercapacitive performance using 3-mercaptopropionic acid*. *New Journal of Chemistry*, 2020. **44**(19): p. 7690-7697.
35. Wang, J., et al., *Electrodeposited cobalt phosphide superstructures for solar-driven thermoelectrocatalytic overall water splitting*. *Journal of Materials Chemistry A*, 2017. **5**(32): p. 16580-16584.
36. Sun, L., et al., *Chemical vapour deposition*. *Nature Reviews Methods Primers*, 2021. **1**(1): p. 5.

37. Yu, S.H. and D.H. Chua, *Toward high-performance and low-cost hydrogen evolution reaction electrocatalysts: nanostructuring cobalt phosphide (CoP) particles on carbon fiber paper*. ACS applied materials & interfaces, 2018. **10**(17): p. 14777-14785.
38. Whittig, L. and W. Allardice, *X-ray diffraction techniques*. Methods of Soil Analysis: Part 1 Physical and Mineralogical Methods, 1986. **5**: p. 331-362.
39. Epp, J., *X-ray diffraction (XRD) techniques for materials characterization*, in *Materials characterization using nondestructive evaluation (NDE) methods*. 2016, Elsevier. p. 81-124.
40. Bunaciu, A.A., E.G. UdrişTioiu, and H.Y. Aboul-Enein, *X-ray diffraction: instrumentation and applications*. Critical reviews in analytical chemistry, 2015. **45**(4): p. 289-299.
41. Holder, C. and R. Schaak, *Tutorial on powder X-ray diffraction for characterizing nanoscale materials*, *Acs Nano*, 13 (2019) 7359-7365.
42. Rostron, P., S. Gaber, and D. Gaber, *Raman spectroscopy, review*. laser, 2016. **21**: p. 24.
43. Qi, Y., et al., *Recent progresses in machine learning assisted Raman spectroscopy*. Advanced Optical Materials, 2023. **11**(14): p. 2203104.
44. Orlando, A., et al., *A comprehensive review on Raman spectroscopy applications*. Chemosensors, 2021. **9**(9): p. 262.
45. Mulvaney, S.P. and C.D. Keating, *Raman spectroscopy*. Analytical Chemistry, 2000. **72**(12): p. 145-158.
46. Mohamed, M.A., et al., *Fourier transform infrared (FTIR) spectroscopy*, in *Membrane characterization*. 2017, Elsevier. p. 3-29.
47. Zhou, W., et al., *Fundamentals of scanning electron microscopy (SEM)*. Scanning microscopy for nanotechnology: techniques and applications, 2007: p. 1-40.
48. Mohammed, A. and A. Abdullah. *Scanning electron microscopy (SEM): A review*. in *Proceedings of the 2018 International Conference on Hydraulics and Pneumatics—HERVEX, Băile Govora, Romania*. 2018.
49. Wang, Z.L., *New developments in transmission electron microscopy for nanotechnology*. Advanced Materials, 2003. **15**(18): p. 1497-1514.

50. Javed, Y., et al., *TEM for atomic-scale study: Fundamental, instrumentation, and applications in nanotechnology*. Handbook of materials characterization, 2018: p. 147-216.
51. Mielańczyk, Ł., et al., *Transmission electron microscopy of biological samples*. Transm Electron Microscope-Theory Appl, 2015: p. 193-236.
52. Zeng, Y., et al., *One-step novel synthesis of Co₂P/CoP and its hydrogen evolution reaction performance in alkaline media*. Materials Chemistry and Physics, 2022. **277**: p. 125419.
53. Doan-Nguyen, V.V., et al., *Synthesis and X-ray characterization of cobalt phosphide (Co₂P) nanorods for the oxygen reduction reaction*. ACS nano, 2015. **9**(8): p. 8108-8115.
54. Yang, X., et al., *Facile and Cost-effective Synthesis of CoP@ N-doped Carbon with High Catalytic Performance for Electrochemical Hydrogen Evolution Reaction*. Chemistry–An Asian Journal, 2023. **18**(20): p. e202300534.
55. Mohammadi, S., M.B. Gholivand, and M. Amiri, *Porous cobalt phosphide nanoflakes supported on ordered mesoporous carbon for superior electrochemical performance supercapacitor and hydrogen evolution reaction*. Materials Today Communications, 2024. **39**: p. 109165.
56. Liang, F., et al., *Microwave-assisted hydrothermal synthesis of cobalt phosphide nanostructures for advanced supercapacitor electrodes*. CrystEngComm, 2018. **20**(17): p. 2413-2420.
57. Liyanage, I.A., H. Barmore, and E.G. Gillan, *Flexible direct synthesis of phosphorus-rich CoP₃ on carbon black and its examination in hydrogen evolution electrocatalysis*. Energy Advances, 2023. **2**(11): p. 1831-1842.
58. Zhang, H., et al., *Controlled synthesis of uniform cobalt phosphide hyperbranched nanocrystals using tri-*n*-octylphosphine oxide as a phosphorus source*. Nano letters, 2011. **11**(1): p. 188-197.
59. Jagadeesh, R.V., et al., *Highly selective transfer hydrogenation of functionalised nitroarenes using cobalt-based nanocatalysts*. Green Chemistry, 2015. **17**(2): p. 898-902.
60. Goyal, V., et al., *Carbon-supported cobalt nanoparticles as catalysts for the selective hydrogenation of nitroarenes to arylamines and pharmaceuticals*. ACS Applied Nano Materials, 2020. **3**(11): p. 11070-11079.
61. Sun, X., et al., *Metal–Organic Framework Mediated Cobalt/Nitrogen-Doped Carbon Hybrids as Efficient and Chemoselective Catalysts for the Hydrogenation of Nitroarenes*. ChemCatChem, 2017. **9**(10): p. 1854-1862.

62. Liu, X., et al., *Single-atom cobalt catalysts for chemoselective hydrogenation of nitroarenes to anilines*. Chinese Chemical Letters, 2023. **34**(12): p. 108745.
63. Xing, L., et al., *A new approach to high performance Co/C catalysts for selective hydrogenation of chloronitrobenzenes*. Journal of Catalysis, 2007. **250**(2): p. 369-372.
64. Yang, J., et al., *Cobalt phosphides nanocrystals encapsulated by P-doped carbon and married with P-doped graphene for overall water splitting*. Small, 2019. **15**(10): p. 1804546.
65. Zhang, Y., et al., *Evaluating the stability of Co₂P electrocatalysts in the hydrogen evolution reaction for both acidic and alkaline electrolytes*. ACS energy letters, 2018. **3**(6): p. 1360-1365.
66. Yang, D., et al., *Synthesis of cobalt phosphides and their application as anodes for lithium ion batteries*. ACS applied materials & interfaces, 2013. **5**(3): p. 1093-1099.
67. Ferrari, A.C. and J. Robertson, *Resonant Raman spectroscopy of disordered, amorphous, and diamondlike carbon*. Physical review B, 2001. **64**(7): p. 075414.
68. Wang, P., et al., *Cobalt phosphide nanowires as efficient co-catalyst for photocatalytic hydrogen evolution over ZnO. 5CdO. 5S*. Applied Catalysis B: Environmental, 2018. **230**: p. 210-219.
69. Qu, Y., et al., *Noble Metal-Coated Cu Nanoparticle Catalysts for Selective Hydrogenation of Nitrobenzene: Modifying Properties of Noble Metal*. ACS Applied Nano Materials, 2024. **7**(16): p. 19457-19465.
70. Li, M., et al., *Origin of the activity of Co–N–C catalysts for chemoselective hydrogenation of nitroarenes*. ACS catalysis, 2021. **11**(5): p. 3026-3039.